10/1-24-94 QSD

SANDIA REPORT

SAND93–2517 • UC–906
Unlimited Release
Printed November 1993

Evaluation of the Electromagnetic Effects due to Direct Lightning to Nuclear Explosive Areas at Pantex

Final Report

K. O. Merewether, K. C. Chen

Prepared by
Sandia National Laboratories
Albuquerque, New Mexico 87185 and Livermore, California 94550
for the United States Department of Energy
under Contract DE-AC04-94AL85000

Issued by Sandia National Laboratories, operated for the United States Department of Energy by Sandia Corporation.

Available to DOE and DOE contractors from
Office of Scientific and Technical Information
PO Box 62
Oak Ridge, TN 37831

Prices available from (615) 576-8401, FTS 626-8401

Available to the public from
National Technical Information Service
US Department of Commerce
5285 Port Royal Rd
Springfield, VA 22161

NTIS price codes
Printed copy: A03
Microfiche copy: A01

SAND93-2517
Unlimited Release
Printed November 1993

Distribution
Category UC-706

Evaluation of the Electromagnetic Effects due to Direct Lightning to Nuclear Explosive Areas at Pantex

Final Report

K. O. Merewether and K. C. Chen
Electromagnetic Analysis and Test Department
P. O. Box 5800
Sandia National Laboratories
Albuquerque, NM 87185-0865

Abstract

This report summarizes the effort to quantify the electromagnetic environments in the nuclear explosive areas at Pantex due to direct lightning. The fundamental measure of the threat to nuclear safety is assumed to be the maximum voltage between any two points in an assembly area, which is then available for producing arcing or for driving current into critical subsystems of a nuclear weapon. This maximum voltage has been computed with simple analytical models and with three-dimensional finite-difference computer codes.

Contents

Contents (Continued)

Illustrations

Acronyms

AWE	Atomic Weapon Establishment
CAD	computer-aided design
CAE	computer-aided engineering
CWIVS	Contaminated Waste Isolation Valve System
DOE	Department of Energy
LPC	Lightning Protection Corporation
MOV	metal oxide varistor
NEA	nuclear explosive area
NRC	Nuclear Regulatory Commission
PVC	polyvinyl chloride
SNL	Sandia National Laboratories
TDR	time-domain reflectometer

Evaluation of the Electromagnetic Effects due to Direct Lightning to Nuclear Explosive Areas at Pantex Final Report

1. Introduction

In a review of the threat to nuclear weapons from lightning surge currents on AC power lines, the Pantex Tester Committee recommended installing AC power line surge arrestors at the AC power entry points of all nuclear explosive areas (NEAs) at Pantex. In a memorandum to Kenneth Pierce, Morris and Chen [1] strongly concurred with that recommendation; however, they also pointed out that surge arrestors limit only the voltage differences between the individual AC power lines, or differential-mode voltages, and that the average voltage of the entire three-wire AC input (and its grounding point) could be raised significantly with respect to other metallic conductors within the bay or cell as a result of a direct lightning strike. This was called "common-mode voltage." The definition was later extended to include the maximum voltage difference between any two points in a bay or cell due to a direct lightning strike, as well as the maximum voltage induced on any single-turn loop formed by walls, roofs, floors, overhead cranes, ducts, pipes, carts, tables, and working fixtures within the assembly area. A recommendation from that memorandum was to conduct a detailed analysis to quantify the common-mode voltages in the bays and cells to determine if there was a threat to nuclear explosive safety. This report summarizes the analysis.

To perform the analysis, every effort was made to determine the maximum common-mode voltage in the NEAs, by considering the worst possible bay and cell construction features, the worst possible lightning protection system, the worst possible attachment point, and a severe one-percent lightning return stroke waveform. The voltages calculated in Sections 7 and 8 are in this sense worst-case upper bounds.

The principal tasks involved in the analysis were to review blueprints of NEAs and perform site visits to Pantex to identify the key electromagnetic features that were considered in the analysis, construct computer models of the cases of interest using commercial CAD/CAE software, calculate the responses using a three-dimensional finite-difference computer code, THREDH, and review NEA procedures to determine whether a threat to nuclear explosive safety exists. Special emphasis, however, was given to developing simple analytical models for the key electromagnetic effects in order to allow the analysis to be extended to other bays and cells at Pantex, and thereby justify that the particular bay or cell chosen for the analysis was indeed the worst case.

1.1 Common-Mode Voltage Mechanisms

Four primary mechanisms produce significant voltages inside reinforced concrete structures. First, metallic penetrations, such as metallic ducts, pipes, or electrical conduits that pass through the wall of an assembly area without being securely bonded to the reinforcing steel at the penetration point, allow the electric field present on the outside of the structure to be transmitted directly to the inside. Thus, a penetration exposed to the near field of an approaching step leader and return stroke would transmit MV/m fields directly into the bay or cell. Second, nearby down conductors carrying lightning currents produce magnetic fields that penetrate the discrete rebar structure and produce voltages on interior loops. These down conductors may be the down conductors of an integral or overhead-wire type of lightning protection system or they may be any other conductor carrying a significant fraction of the lightning current. Third, inadequate bonding of the reinforcing steel in the roof, walls, and floor forces lightning currents to flow through

concrete or other resistive joints to produce voltage differences that are potentially higher than those due to any other mechanism. Fourth, the flow of lightning current on the walls of the structure produces an inductive voltage drop, which is then available for driving interior circuits. Lightning current is produced on the walls of the structure directly, when an air terminal connected to the reinforcing steel is hit by lightning, and indirectly, when an image current is induced on the reinforcing steel due to the flow of lightning current some distance away.

With respect to the first mechanism, penetrations have the potential to produce the highest electric fields in the bays and cells; however, they do not require detailed analysis, because it is fairly easy to reason that any electric field present outside the structure will be transmitted directly to the inside. It is a recommendation of this report that a penetration tester be developed to ascertain the effectiveness of the bonds where metallic penetrations enter the nuclear explosive areas. Second, down conductors that pass very close to cavity walls are also capable of generating significant interior voltages through magnetic-field coupling to loops; however, an examination of the plans and the application of simple analytical formulas leads to the conclusion that all down conductors are sufficiently far away from the assembly areas that the resulting voltages (both the early and late time components) are smaller than those due to inductive drops along the wall. Third, no bonding deficiencies were identified in the drawings that would lead to significant resistive voltage drops. A separate report by Seely and Holmes [2] showed that the contact resistance of a typical rebar junction is negligible compared to the inductive reactance of a typical wall. Therefore, the task is to identify the particular bay and cell that is expected to produce the maximum inductive voltage drop from lightning current flowing on the walls (mechanism 4).

2. Summary of Analysis and Test

Laboratory testing was performed of the Lightning Protection Corporation (LPC) arrestors in a configuration electrically equivalent to that in NEAs (with MOVs simulating the front end of an AC tester and an LPC arrestor in the electrical room). When the power distribution lines on the secondary of the transformer in the electrical room were subjected to typical 8-kV and 25-kV lightning surges, the input voltages at the AC testers were limited to a few hundred volts [3]. This clearly demonstrated the efficacy of the surge protection.

In a worst case, when lightning strikes air terminals or other protrusions (e.g., vents) directly, the maximum voltages between different points of the building are calculated to be 3 kV for a bay, 10 kV for a cell, and 100 kV for the ramp. It is unlikely that these voltages in the bays and cells will cause safety concerns; and because the partially assembled weapons are enclosed in shipping containers in the ramps, the higher-voltage value in the ramp does not cause safety concerns, either. Of greater concern is a metallic conductor entering the bay or cell interior if the conductor is not bonded to the wall rebar at the penetration point. This issue is addressed in the recommendations.

3. Recommendations

The present analysis and tests demonstrate that direct-lightning strikes to air terminals or overhead ground wires do not cause significant voltages on conductor loops inside the NEAs. By avoiding connecting the weapon assembly electrically to the static ground bus, the potentially large voltage (a few kVs) induced on the rebar cannot directly couple to weapon subsystems. Nuclear weapon assembly at Pantex is extremely safe from the abnormal lightning environments. The following recommendations are compiled not because any safety problems have been identified, but rather to enhance further the safety of these operations.

Because penetrations have the potential for producing the highest electric fields in the bays and cells, and because bonding at penetrations cannot be determined by visual inspection, it is recommended that a penetration tester be developed to ascertain the effectiveness of the bonds where metallic penetrations enter the nuclear assembly areas. A time-domain reflectometer with an appropriate current source can be used to determine the quality of the junction of the penetration and the wall rebar.

With proper installation of the LPC arrestors and tester MOVs, AC testers are no longer a safety threat during a lightning storm. It is recommended that during static alert and lightning storm alert, use of AC testers at the NEAs be allowed. However, strict observance of static alert and lightning storm alert restrictions should remain in effect for Building 12-64, where the LPC arrestors are not yet installed.

Because older sections of the NEAs are not protected by overhead ground wire lightning protection systems, it is recommended that Pantex and SNL jointly design an overhead ground wire system for optimum protection against lightning. A poorly designed overhead ground wire protection system may not provide an improvement over an air terminal system. A very well designed overhead ground wire protection system can reduce the voltage coupling to the interiors of bays and cells by as much as a factor of ten. When a design is available for erecting an overhead wire protection system, Pantex should proceed with the installation of such a system over the older section of NEAs. Enhanced safety to the NEA operation during a lightning storm should be well worth the minimal cost for such an installation.

Lightning protection systems used in the U.K. and in the U.S. DOE complex were compared during a joint conference held June 21 through 25, 1993, at Pantex and which involved representatives of SNL, Pantex, and the Atomic Weapon Establishment (AWE), Burghfield, England. At the AWE, all conducting structures are connected. The counterpoise buried ground wires of the overhead lightning protection system are connected at many locations to the building rebar, which are in turn connected through the conducting floor to the technicians and to the partially assembled weapon. At Pantex, the counterpoise buried ground wires are connected to bays and cells indirectly through the static grounding grid. The technicians are bonded only to the local object under assembly; because Pantex floors are not conducting, there is no direct conducting path from the counterpoise ground wire to the technicians or to the partially assembled weapon.

Although both Pantex and the AWE practices are sound, an investigation jointly by Pantex (with SNL) and the AWE should be conducted to document the technical justifications for the practices. Furthermore, this investigation should enhance the electromagnetic safety at Pantex and at the AWE.

4. Characterization of the Lightning Threat

The lightning process begins with an electrically neutral cloud. Falling precipitation formed at higher altitudes collides with water droplets in the warmer, rising portions of the cloud. These collisions result in a transfer of electric charge between the two bodies, and over time, the cloud is eventually polarized. Usually, the base of the thundercloud is negatively charged and results in negative lightning, i.e., a lowering of negative charge to the earth. The polarization of charge in the thundercloud gives rise to an image charge in the earth by driving away electrons from the surface. The electric field in the region between the negatively charged base of the cloud and the positively charged surface of the earth continues to increase as the cloud becomes more and more strongly

polarized. When the local electric field at a point near the base of the cloud exceeds the dielectric strength of air, a thin conducting channel is formed, called a pilot leader. The conductance of the channel allows charge to flow freely to the tip of the leader, where again the dielectric strength of air is exceeded and dielectric breakdown occurs. This process proceeds toward the ground with distinct steps, which have a pronounced vertical component but in general a random direction in space. The final attachment point of the lightning strike is not determined until the last one or two steps of the stepped-leader process, at which point the electric field between the tip of the stepped leader and object being struck is strong enough to initiate an upward streamer from the eventual point of strike. When the upward streamer and downward leader meet, the charge stored on the stepped-leader flows to the earth by means of a wave like disturbance that begins at the earth and propagates upward toward the cloud. This is called the first return stroke. As a result of the initial ionization process, a preferential path is established between the cloud and ground for perhaps several subsequent return strokes. A lightning flash is the total event, including the stepped-leader process, first return stroke, and all subsequent return strokes.

The rise time, fall time, and peak amplitude of the current wave form resulting from a return stroke vary according to a log-normal distribution, i.e. a Gaussian distribution with respect to the logarithm of the variate. The probability density function for the peak amplitude is of the form,

$$f(I) = \frac{1}{\sqrt{2\pi}\sigma} e^{-\frac{1}{2}\left[\frac{\log I - \log \bar{I}}{\sigma}\right]^2},$$

where the mean $\bar{I}$ and standard deviation σ that best fit the entire range of peak stroke amplitudes are 30 kA and 0.32, respectively, with 200 kA occurring at about the one-percent level. While a return stroke is normally classified according to its peak amplitude, with a severe stroke considered to be 200 kA, for the purposes of this report, the time derivative of the lightning current $\partial I/\partial t$ is a more relevant parameter, the maximum measured value being 360 kA/μs [4,5]. As an aside, the return strokes that exhibit the maximum rates of rise are not the same return strokes that produce the 200-kA peak amplitudes. The former are associated with negative subsequent return strikes, while the latter are associated with positive lightning, which generally have longer rise times.

5. Pantex Plant, General

The Pantex plant is located near Amarillo, in the central Texas panhandle at 35° latitude. The site measures 5 miles in the east-west direction and about 3.5 miles north to south, for a total area of 45.3 km^2. It is organized into zones. Zone 12 is where assembly and disassembly operations are performed and is approximately 1800' by 2600', or 0.43 km^2, in area.

The top 60 to 80 feet of soil is classified as "Pullman silty clay loam." Ground conductivity maps produced by the Federal Communication Commission show that the soil conductivity is 0.015 S/m and relatively uniform.

Estimates of the average number of thunderstorm days per year at the Pantex plant differ by almost a factor of two. According to the World Meteorological Organization [6], the average number of thunderstorm days per year, T_y, at Amarillo is 38; according to the U.S. Weather Service [7,8], T_y is 40; according to the National Fire Protection Association [9], T_y is 50; and according to the Nuclear Regulatory Commission [10], T_y is 60. The NRC isokeraunic map for the contiguous 48 states is shown in Figure 1. The total annual lightning flash density τ_y, in fl/km^2/yr,

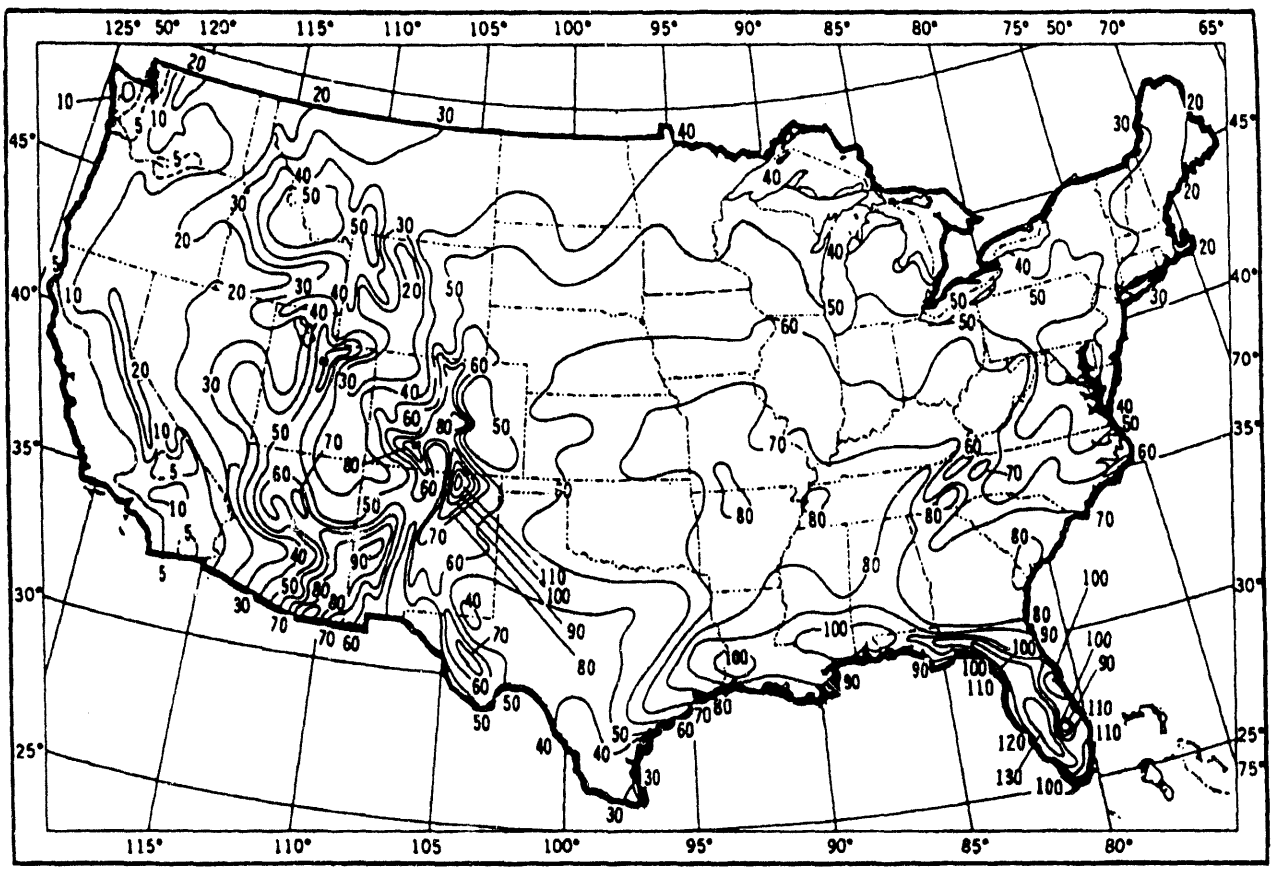

Figure 1. Isokeraunic map showing the average number of thunderstorm days per year for the contiguous 48 United States [10]

including both cloud-to-cloud and cloud-to-ground flashes, is described by the empirical formula [11].

$$\tau_y = 0.02 T_y^{1.7} .$$

The fraction of the total lightning activity that results in cloud-to-ground flashes depends on latitude, λ, according to the formula [11]

$$P = 0.1\left[1 + \left(\lambda/30\right)^2\right],$$

where λ is in degrees. Therefore, the ground flash intensity N_g, in fl/km²/yr, is given by

$$N_g = P\tau_y .$$

Substituting yields a total flash density ranging from 9.7 to 21.1 fl/km²/yr for isokeraunic levels of 38 and 60, respectively; 23.6 percent of the total are cloud-to-ground flashes; therefore, the ground flash density N_g is 2.3 to 5.0 fl/km²/yr. The number of lightning flashes expected in a given region can be estimated by multiplying the ground flash density by the area of the region. The expected

number of flashes to the Pantex site, for example, ranges from 104 to 226 flashes/yr, which is consistent with data from the local lightning detection system at Pantex (see Appendix A). The expected number of flashes to Zone 12 is 1.0 to 2.2 flashes/yr.

During a snowstorm in January 1986, lightning hit a transformer on an overhead pole near Building 11-54. Since 1988, all exterior power distribution wiring from transformers to power distribution panels has been converted to buried wires. The latest incident occurred in September 1992, when lightning struck the ground near a guard shack in Zone 12.

Generally speaking, Zone 12 consists of bays and cells, where assembly and disassembly operations are conducted, and an interconnected network of enclosed corridors, called ramps, for the passage of nuclear weapons and personnel. The bays are rectangular reinforced concrete rooms, where all operations are permitted except those involving the lowest configurations of nuclear weapons with conventional high explosive. These latter operations are performed only in the cells, or gravel girties, which are round rooms with reinforced concrete walls and floors and a circuitous system of corridors connecting the round room to the ramp to dissipate blast energy. The site also contains numerous buried magazines for intermediate-term storage of completed weapon assemblies and partially assembled weapons in shipping containers, and a small fleet of hardened trailers to move the weapons between the material access areas in Zones 12 and 4. A detailed lightning analysis of the storage magazines and safe secure trailers, including the lightning protection systems for loading and unloading operations, is beyond the scope of this report, which is concerned primarily with the ramps, bays, and cells.

5.1 Ramp Construction — Key Electromagnetic Features

Ramp construction varies throughout the plant; however, most of the ramps share the features shown in Figure 2. The ramp is built on a 1-ft-wide reinforced concrete footing with a 6-in-thick reinforced concrete floor. The walls consist of vertical I-beams, at 20' intervals on center, and horizontal channel girders, covered by 1-5/8" thick panels of cement-asbestos siding. In some areas, one wall of the ramp is of I-beam construction, and the other wall is a reinforced concrete retaining wall for a common earth overburden. The vertical I-beams are nominally 8" deep, with 4-in-wide flanges, while the horizontal channel girder is 6" wide and is mounted typically 4'-6" above the finished floor. The transverse framing members of the roof are also 8-in-deep steel I-beams, which support 5 or 6 steel purlins that run the full length of the ramp. The roof is decked with cement-asbestos sandwich panel and covered with aluminum roofing. The outside dimensions of the ramp are typically 12' to 14'-6" wide by 12' high at the peak. There is a minimum of 8'-3" clearance from the finished floor to the bottom of the pipe supports.

5.2 Bay Construction — Key Electromagnetic Features

5.2.1 Bay Selection

As stated previously, the focus of this analysis estimates the common-mode voltage drop due to the flow of lightning current on the bay walls. Because the 12-84 W, 12-99, and 12-104 bays are protected by an overhead-wire lightning protection system, the lightning currents flowing in the walls and floors of these bays should be much lower than the currents in the walls of the 12-64 and 12-84 E bays due to a similar lightning flash. The construction of Building 12-84 E (4' 6"- thick, laced reinforced concrete walls) is such that the effective sheet inductance is very small, resulting in low field levels in these bays also. The worst case is a 12-64 bay, which is protected by an

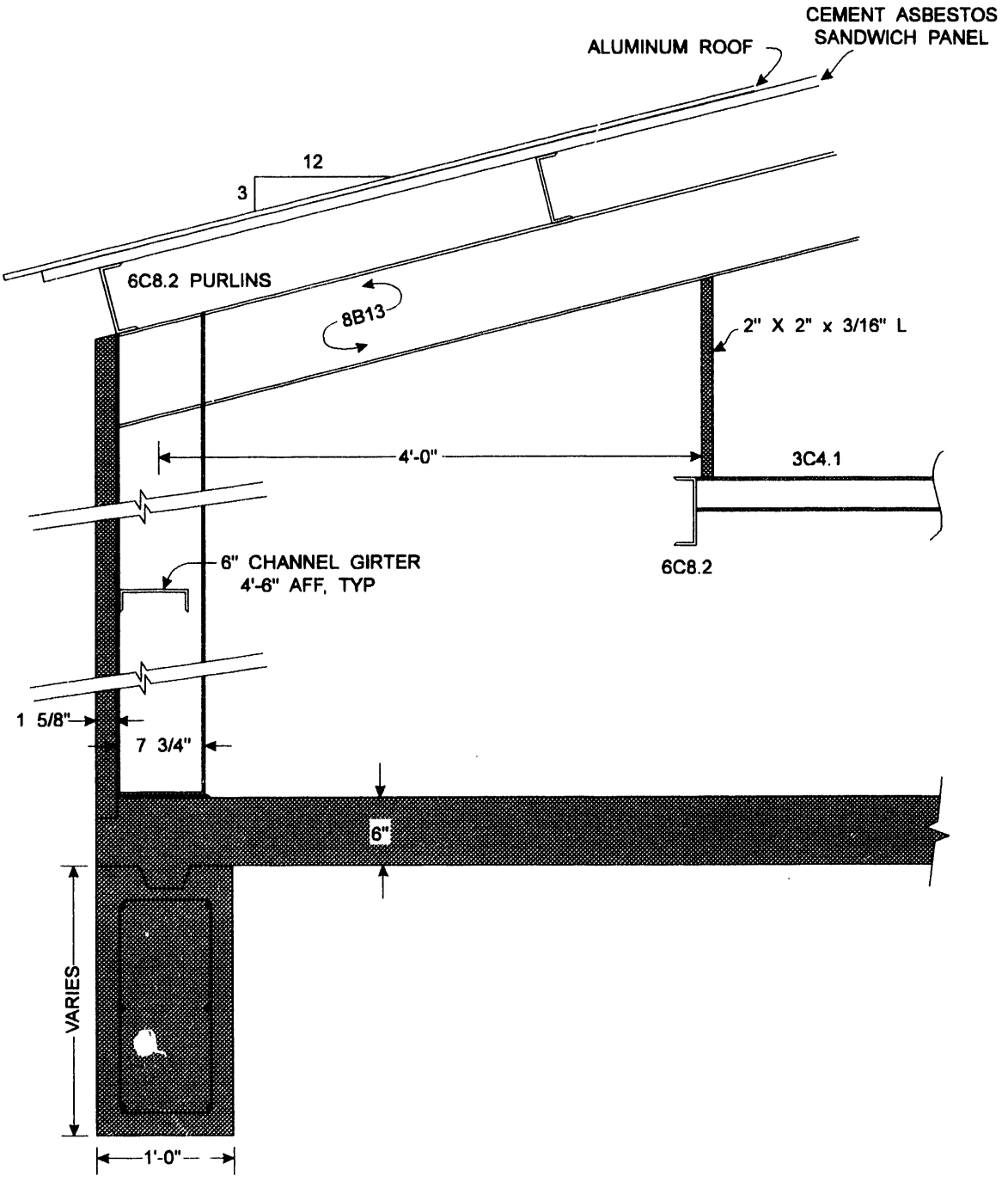

Figure 2. Typical ramp construction features

integral type of lightning protection system (air terminals, primary down conductors, ground-ring electrodes, and ground rods), which results in a significant fraction of the total lightning current flowing on the reinforcing steel in the walls. Furthermore, the design of the reinforcement in the walls should provide a higher inductance than that of Building 12-84 E. A cross section through the 12-64 bay complex is shown in Figure 3.

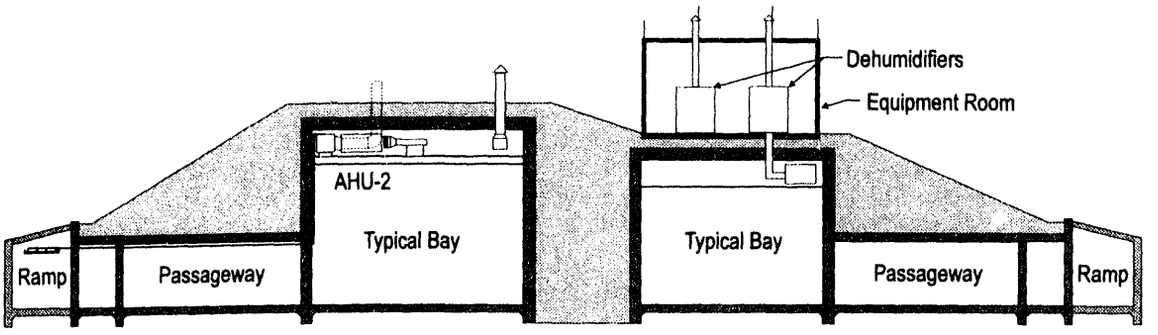

Figure 3. Cross-sectional view of the 12-64 bay complex

5.2.2 General Structural (D12-64A5)

The 12-64 bay complex consists of small and large bays arranged in two rows, separated by 19' of compacted earth fill. Adjacent bays are separated by 13'-6" and covered by 2' of earth fill. Bays 1 through 9 are 24' by 28' by 19' (inside dimensions); bays 10 through 17 are 28' by 30' by 23'. The walls are concrete, 18" thick, with two layers of simple (unlaced) reinforcement as shown in Figure 4. The roof is constructed of two reinforced concrete panels that taper from 18" thick at the walls to 9" thick at the centerline. The floor is also 18"-thick reinforced concrete. The roof and walls are covered by a 4"-thick layer of polystyrene, which is not present under the floor. The whole 12-64 complex is covered with a 3" layer of Gunite and a layer of Gulfseal waterproofing material. The bay is connected to the ramp by a single passageway with 8' by 8' by 4"-thick interlocked steel blast doors at both ends.

Two adjacent bays share a common dehumidifier house, which houses the dehumidifier units for the two bays. The dehumidifier house has a 15'-6" by 18'-6" concrete foundation and floor, reinforced with #3 rebar spaced at 15" each way. The frame consists of four 8-in-nominal-depth steel I-beams located at the corners of the structure, strengthened by 1/2" diameter cross bracing. The siding is 1-9/16" thick asbestos sandwich panel. The roof is cement-asbestos paneling covered with aluminum roofing.

Each bay is equipped with an overhead crane, with a minimum of 3'-0" of clearance between the crane and the roof. The crane is well bonded to the reinforcing steel in the walls.

5.2.3 Air Conditioning Ducts and Piping (D12-64M3, D12-64M4)

Each dehumidifier unit has a large diameter ventilation duct that penetrates the roof of the dehumidifier house and is exposed to direct lightning. From the dehumidifier unit to the bay, there are two large-diameter ducts for dry air supply and moist air return (14"-diameter ducts for the small bays, and 16"-diameter ducts for the large bays) that pass through the floor of the dehumid-ifier house and into the bay through steel sleeves in the bay wall. These ducts have heavy canvas vibration isolators, which may or may not have flexible copper jumpers installed across them. Near one corner of the bay is an exhaust vent that passes through a sleeve in the roof to the outside and is also exposed to direct lightning. The center of the vent is 1' from the inside surface of the back wall and 1'-6" from the inside surface of the side wall of the bay. The air

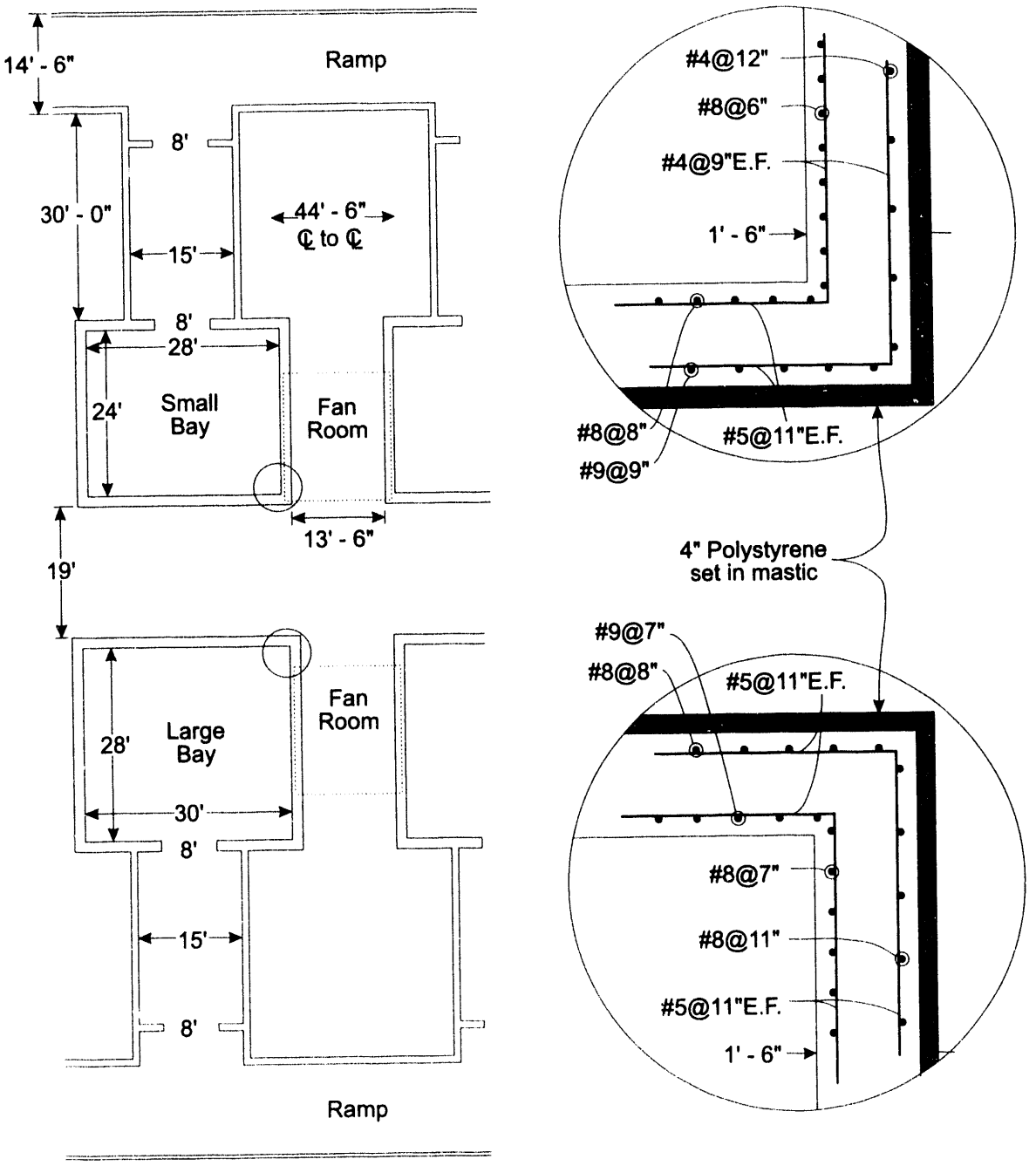

Figure 4. Plan view of Building 12-64 bays, showing reinforcement details in the walls

conditioning unit for a 12-64 bay is located between the ceiling and the roof and is supplied by 1-1/2"-diameter chilled water and chilled water return pipes that pass through the airlock from the ramp. At the bulkheads above the blast doors, the pipes pass through steel sleeves in the walls, with lead-wool caulking. On the roof, mounted on H-frame supports are two steam pipes that taper from 2" in diameter near the equipment room to 1" in diameter, with a 1" service to each of the dehumidifier houses.

5.2.4 Lightning Protection and Static Bonding System

The lightning protection system for the 12-64 bays is an integral system, consisting of air terminals, down conductors, and a continuous buried ground ring electrode around the perimeter of the 12-64 complex. Details of the lightning protection and static bonding system are shown in Figure 5. On each corner of the dehumidifier rooms and on both dehumidifier vents are 2' air terminals, which are interconnected by a loop of stranded aluminum lightning cable. Two down conductors at two opposite corners of the dehumidifier room connect the air terminals to a 1'-deep buried ground ring electrode that encircles the dehumidifier room. Between the two rows of bays are two #1/0 primary lightning conductors that run the entire length of the complex, buried 1' below the surface. These primary lightning conductors connect to the dehumidifier room ground electrodes, and to 5'-tall air terminals on the exhaust vents of each bay. At 88'-100' intervals, #1/0 buried conductors connect these central lightning conductors to the lightning protection system on the ramp, consisting of a row of air terminals on top of the retaining wall and a row of air terminals along the outside edge of the ramp, interconnected by stranded lightning conductors. The air terminals are spaced at 20' intervals along the ramp, and connections between the two rows of air terminals are provided every 80' along the ramp. Down conductors every 20' connect the outer lightning protection cable to the bare copper counterpoise, buried 3' below finished grade.

A #1/0 basketweave copper ground bus is mounted on the inside surface of the bay walls, 40" above the finished floor, and is bonded at one location to the reinforcing steel in the foundation with a cable-to-steel thermoweld connector. At this point, a connection is provided to a bare copper static ground wire, midway between the two rows of bays, 3'-0" below floor level.

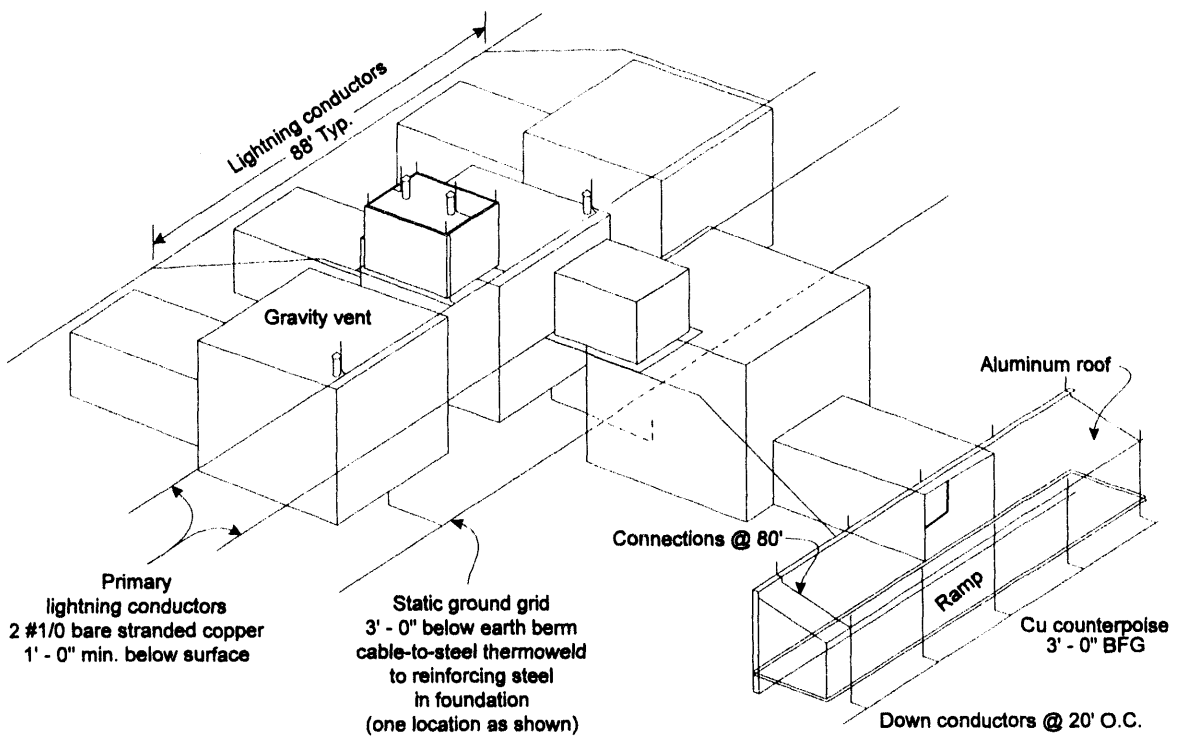

Figure 5. Lightning protection and static grounding system for Building 12-64

5.2.5 High-Explosive Contaminated Water Disposal

Hot water is used to dissolve high explosives in bays 16 and 17. Hot water supply and hot water return pipes are routed from the 12-64 equipment room to bays 16 and 17 in 1"-diameter pipes mounted on pipe supports, spaced 10' on center. Waste water is pumped from the bays through 2"-diameter above-ground water pipes to a tanker truck located some distance from the ramp. The 2"-diameter pipes pass through drilled holes in the concrete walls above the blast doors, across the ramp to the outside, up to a height of 12', and thence to a tanker truck 80' away. The waste water pipes are supported by concrete anchors and pipe hangers in the interlock, by beam clamps and pipe hangers in the ramp, and outside by 3"-diameter pipe supports, set in 36"-deep concrete at 10' intervals.

5.2.6 Fire Protection System (D12-64F2, D12-64-F2.1, D12-64F2.2, D12-64-F2.3, D12-64F4, D12-64-F4.1)

Zone 11 and Zone 12 South are served by a high-pressure fire-protection network that generally consists of 10" cast iron pipe for the main distribution pipes, 8" pipe for the secondary branches, and 6" cast iron pipe to the mechanical rooms of the bays and cells. These pipes are 48", minimum, below ground level. At the equipment room, the 6" pipe makes a 90° elbow and enters the equipment room through the floor. From here, the pipe enters a riser/alarm valve that feeds a 5"-diameter fire main which encircles the 12-64 complex to serve all of the 12-64 bays and interlocks. This 5" loop is routed through the ramp, near the roof, 3'-6" from the retaining wall. At each interlock, a 2-1/2" diameter pipe emerges from a tee in the 5" line and passes through 4"-diameter pipe sleeves in both of the interlock walls, 9' 5-3/4" above the finished floor. Once in the bay, the pipe follows the bay wall toward the ceiling until it is 30" below the bottom of the deck. From this point, it serves 10 (small bay) or 12 (large bay) sprinkler heads mounted approximately 35" below the concrete deck, on 1"-diameter pipe. These pipes are supported by 12 to 16 3/8" hangers, and, presumably, by concrete anchors. As a result of a fire-protection upgrade, a 2" loop was added for the ramp with sprinkler heads at 10' on center.

5.2.7 Lighting (D12-64E6)

Electrical conduits for the 12-64 lighting circuits originate in lighting panels between bays 4 and 5 (for the south row of bays) and between bays 13 and 14 (for the north row). In general, 1" conduits are used for both the ramp lighting circuit and for the bay lighting circuit, although slightly larger conduits are required near the lighting panels to accommodate a larger number of wires. From a junction box near the interlock door, the conduit passes through a penetration in the concrete wall above the door. It travels down the center of the interlock, supplying power to a small number of fluorescent fixtures, and enters the bay through a second penetration in the opposite interlock wall. Once in the bay, it supplies a large number of fluorescent fixtures through several metallic conduits.

Lights for the dehumidifier houses are supplied by 1" metallic conduit, routed alongside the steam pipes. These conduits terminate in a lighting panel on the outside wall of the ramp between bays 13 and 14.

5.2.8 Fire Alarm and Public Address System

The two main conduits for the fire alarm and public address systems run the full length of the 12-64 ramps. The fire alarm conduits do not enter the bays. The public address system conduit enters the bay through the interlock and feeds a public address speaker on the nearest interior bay wall.

5.3 Cell Construction — Key Electromagnetic Features

5.3.1 Cell Selection

The 12-85, 12-96, and 12-98 cells are all protected by an overhead-wire lightning protection system, and the currents flowing in these cell walls will be substantially lower than the currents in the 12-44 walls, which are protected by the integral type of lightning protection system. There are vo potential strike points on the 12-44 cells: the intended strike point on air terminals on steel ventilation ducts, and an unintended strike point to the top of the gravel mound, which is not within the protected zone of the lightning protection system. Because of the possibility that conducting channels through the gravel may exist (formed by roof leaks, root formation, roof-mounted piping, etc.), it is very difficult to assign a reduction factor to estimate the fraction of the lightning current reaching the cell. It must therefore be assumed that the full lightning current reaches the cell and is injected at the worst possible point. The unintended strike point therefore results in the greatest fraction of the total lightning current flowing on the cell walls and the greatest voltages inside the round room. The ventilation ducts are securely grounded to the reinforcing steel in the roof of the equipment room, which will effectively drain the lightning current away from the round room.

5.3.2 General Structural

There are six assembly cells in the 12-44 complex, separated by a nominal spacing of 80' center-to-center. The cells are characterized by a 34'-diameter round room and a circuitous system of corridors and gravel pockets to dissipate blast energy before it reaches the doors in the event of an internal explosion. The walls of the round room are 21'-6" tall from the top of the finished floor, and are made of 12"-thick concrete, reinforced by two layers of 1/2" diameter steel bars. The vertical rebar is spaced at 12" on centers; the horizontal rebar is spaced at 18" on centers. The floor of the round room is 6"-thick reinforced concrete. The roof consists of an 18" by 18" mesh of 1-1/2"-diameter bridge strand cable, suspended from a ring beam at the top of the room, and four layers of 2" by 2" #10 AWG woven wire mesh supporting a 19'-thick layer of gravel (nominal thickness). The gravel mound is capped with a 3" layer of Gunite, reinforced with woven wire mesh, and reaches a maximum height of 15'-6" above the ring beam, which brings the total height of the structure to 37' above ground level. There are two additional layers of 2" by 2" #10 AWG woven wire mesh embedded in the gravel five feet above the primary roof support. The cell is surrounded by a massive volume of earth fill, which extends approximately 84' from the center of the cell. Elsewhere in the cell, the roof, walls, and floor are 18" thick and reinforced by two layers of 1/2"-diameter steel bars at 12" on center each way. The term cell is describes the round room, equipment room, staging and storage areas, and all interconnecting corridors. A sketch of a typical 12-44 cell is shown in Figure 6.

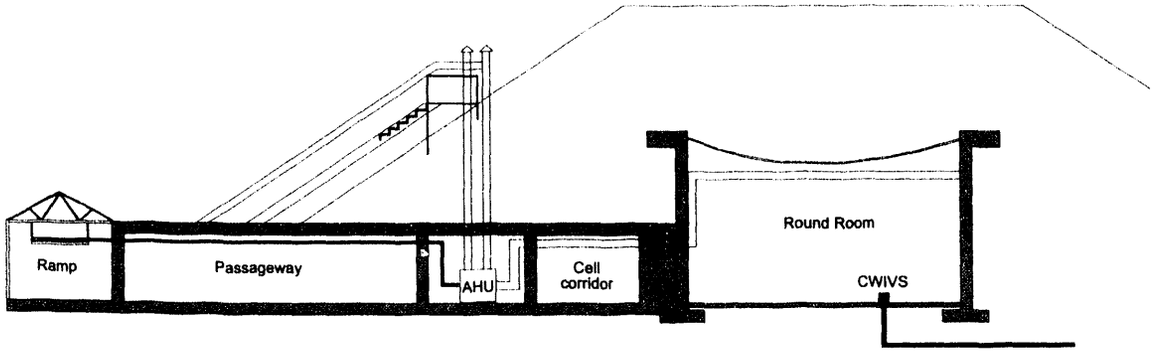

Figure 6. Cross-sectional view of a 12-44 assembly cell

The round room is equipped with two overhead jib cranes, which are bonded to the reinforcing steel in the walls by means of Cadweld connectors and #1/0 AWG bare copper cable. Personnel access to the cell is through a 5'-6" rotating steel door.

5.3.3 Air Conditioning Ducts and Piping (D12-44M2)

The air conditioning unit for the 12-44 cells is located in a 10' by 12' mechanical equipment room near the entrance to the cell. It is connected to a fresh air intake duct, an exhaust duct, and the interior ductwork inside the cell. The exterior duct closest to the round room is the fresh air intake duct, which makes two 90° bends between the equipment room and the surface such that the separation between intake and exhaust vents is 2' at the equipment room and 8' at the surface. It is made of 10"-diameter 10-gauge welded steel pipe, extending 24" above the surface of the fill, and is wrapped with Polyken 920 protective tape. At the equipment room, the intake and exhaust ducts pass through a 24"-long cast-in-place flange spool, which is well bonded to the reinforcement in the roof. The exhaust vent, which also makes two 90° bends between the equipment room and the surface, is 12"-diameter 12-gauge welded steel pipe, extending 10' above the surface. It is also wrapped with Polyken protective tape.

The interior supply duct is connected to the vertical climate changer by a heavy canvas vibration isolator and passes through a steel sleeve in the equipment room wall to the cell corridor. The duct is principally 34" by 14" as it winds through the corridors to the round room, at which point it divides into two branch ducts that feed four diffusers in the ceiling. In the corridors, the bottom of the duct is 7'-2" above the finished floor, while in the round room, it is 16'-0" above the floor. All ducts are supported by pipe hanger inserts on 5' centers.

The air conditioner is served by two 1-1/2" chilled water supply and chilled water return pipes, which enter the cell through the equipment passageway. Other penetrations into the cell include a 1-1/2" condensate pipe, 1-1/2" steam line, 1-1/2" vacuum line, 3/4" air line, and carbon dioxide piping. These pipes pass through sleeves in the concrete walls above the blast doors, 7'-10" above the finished floor, to connections in the adjoining ramp. The sleeves are caulked with lead wool caulking.

In the ramp, the chilled water supply and chilled water return pipes are typically 3" in diameter, the steam pipe is 4", the vacuum pipe is 2", and the air line is 1-1/4" in diameter. These pipes originate in the 12-44 E central equipment room and are hung from angles with split ring connectors every 10'.

5.3.4 Dehumidifier Unit and Ductwork

The dehumidifiers for the 12-44 cells are located on the roofs of the equipment passageways. They are mounted on two treated 6 by 6's anchored to the concrete at 42" center-to-center. The dehumidifier is connected to the fresh air intake duct through a 12-gauge 12"-diameter duct, whose maximum length is 71'-8" (cell 5). The dehumidifier receives its power through a 3/4" electrical conduit; otherwise, the grounding of the dehumidifier is not known.

5.3.5 Lightning Protection and Static Bonding System

The 12-44 cells are protected by an integral lightning protection system. Air terminals are mounted to the two exterior ventilation ducts, which are connected by down conductors to a #1/0 AWG buried counterpoise, 3' below grade and 3' from the cell walls. The counterpoise is connected periodically to 10'-long copper ground rods. The doors are securely bonded by 1"-wide flexible copper bonding straps to the door frames, which are themselves bonded to the reinforcing steel in

the walls. Each cell is equipped with a #1/0 basketweave copper ground bus, 40" above the finished floor.

5.3.6 Fire Protection System

Zone 11 and Zone 12 south are served by a high-pressure fire protection system that consists of 10" main distribution piping, 8" secondary piping, and 6" connections to the facilities. The fire protection piping is buried 48", minimum, below finished grade. There is a 6" cast iron connection at the 12-44E central equipment room that serves the automatic sprinkler system in the 12-44 cells. The fire protection piping is 6" in diameter in the 12-44 ramp, 8'-2" above the floor, and it is 5" in diameter in the cells, 7'-10" above the floor. The round room is protected by both an automatic deluge sprinkler system and a wet-pipe system. The deluge system in the round room is below the suspended ceiling and has 16 heads. The wet-pipe system in the round room is located above the ceiling and has 12 heads.

5.3.7 Contaminated Waste Isolation Valve System

If fire fighting water is discharged in a cell, the potentially contaminated water is collected by the Contaminated Waste Isolation Valve System (CWIVS) to prevent it from being discharged to the environment. The CWIVS piping is 6"-diameter PVC, in a 50' steel sleeve at the cell. The pipe is buried 30", minimum, below finished grade. Potentially contaminated water is discharged to a 20,000-gallon holding tank.

5.3.8 Power Distribution Conduit

The conduits identified in the review of the blueprints include: (1) a 3"-diameter underground conduit, 60' long, from a pad-mounted transformer to 12-44E, (2) a 1-1/4" conduit, 160' long maximum, from 12-44E through the ramp to power distribution panels in the cells, (3) 3/4" conduit to the dehumidifier, and (4) 1/2" conduit to a sump pump in the mechanical room of the cell .

6. Analytical Estimates

6.1 Approach

Having eliminated all other sources, the voltages inside the nuclear explosive assembly areas can be characterized by the sheet inductance of the reinforcing steel in the roof, walls, and floor. As a general rule, for structures in which the lightning protection system is intimately bonded to the reinforcing steel of the building, the resistive effects associated with the soil, concrete, and structural steel members play a lesser role in determining the interior electric fields and voltages. In a separate report, Seely and Holmes [2] measured the contact resistances at typical rebar junctions and concluded that the resistive voltage drop along a reinforced concrete wall was indeed negligible compared to the inductive voltage drop. Many of the most important effects from the standpoint of safety can be predicted by the application of simple circuit models and later validated and refined by full three-dimensional numerical simulation tools. The approach here is to postulate worst-case source and sink points for the lightning current on a structure that houses a partially assembled nuclear weapon, estimate the effective inductance of the structure, then determine the maximum open-circuit voltage appearing inside the structure due to a severe lightning return stroke.

Sheet inductance is a very useful concept for estimating the dominant voltage drop due to the flow of lightning current in layers of reinforcing steel in a concrete wall. The sheet inductance

formula used in the following sections is based on the low-frequency surface impedance of a grid of long parallel cylindrical conductors [12]:

$$L_S = \frac{\mu_0}{2\pi} s \ln\left(\frac{s}{2\pi a}\right) \text{H / sq}$$

where s is the spacing and a is the radius of the conductors. Note that the sheet inductance L_S has units of H/sq; for a uniform current distribution, the inductance L_S^{tot} to be used in an equivalent circuit model is obtained from L_S by multiplying by the length and dividing by the width of the current sheet. Once the effective inductance is known, the maximum open-circuit voltage appearing inside the structure is estimated from the formula

$$V_{oc}^{\max} = L_S^{tot} \left.\frac{\partial I}{\partial t}\right|_{\max}$$

6.2 Ramp Analysis

The type of ramp that is expected to yield the worst-case voltage is of steel I-beam construction for the roof and both walls. The large number of horizontal I-beams, steel trusses, conducting pipes, and conduits allow the roof to be adequately approximated by a perfectly conducting sheet; the vertical I-beams result in a shunt inductance to ground. Neglecting all resistive effects and the inductance of the reinforcing steel in the floor, the equivalent circuit for a long section of ramp can be approximated by the inductive ladder network shown in Figure 7, where it is assumed that lightning attaches to an air terminal near one of the vertical I-beams.

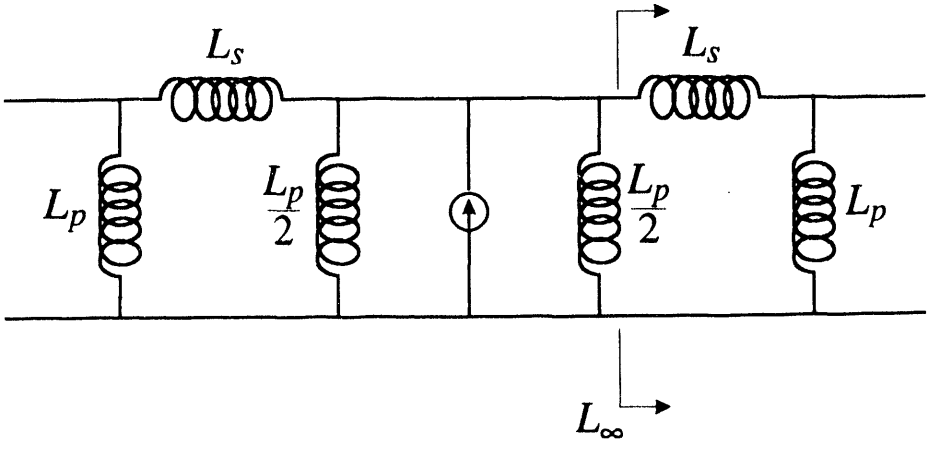

Figure 7. Conservative ladder network model for the ramp analysis

L_S is the series inductance associated with the ramp roof, and L_p is the parallel inductance of the vertical supports. The circuit elements are approximated by the formulas:

$$L_s = \mu_0 \frac{h}{w} s$$

$$L_p = \frac{1}{2}\frac{\mu_0}{2\pi} h \ln\left(\frac{s/2}{a_{eff}}\right),$$

where h and w are the height and width of the ramp, respectively, s is the spacing between the vertical I-beams, and a_{eff} is the effective radius of the vertical I-beam supports (note that L_s neglects the compensating effects due to the transverse inductance of current on the underside of the roof and the inductance of the top of the roof to ground). From the ladder circuit model, the total input inductance of the network is

$$L_{in} = \frac{1}{2}\left[\frac{\frac{L_p}{2} L_\infty}{\frac{L_p}{2} + L_\infty}\right],$$

where,

$$L_\infty = \frac{1}{2}\left[L_s + \sqrt{L_s^2 + 4 L_s L_p}\right].$$

Substituting h = 10 ft, w = 13.5 ft, s = 20 ft, and a_{eff} = 1.5 in. yields a total input inductance of 0.30 μH, and a maximum open-circuit voltage,

$$V_{oc} = L_{in} \left.\frac{\partial I}{\partial t}\right|_{\max} = 109.4 \text{ kV}.$$

The two I-beams near the source carry 91 percent of the total current.

6.3 Bay Analysis

Incorporating a better knowledge of the 12-64 bays, the analysis in this section differs from the analysis presented in an earlier report [13]. For this analysis, it is assumed that the point of strike is on the isolated exhaust vent at the corner of the bay. Because of the 4"-thick polystyrene layer on the bay roof and walls, significant lightning currents can reach the bay only by means of the ventilation ducts. According to the drawings, no other conductors penetrate the polystyrene layer. There are therefore two possible attachment points: on the exhaust vent in the corner of the bay, and on the dehumidifier house. A strike to the dehumidifier house would not produce the worst-case voltage for several reasons: first, assuming good electrical bonding in the dehumidifier room, the current would be shared between two adjacent bays, rather than being injected onto a single bay; and second, if the two dehumidifier units were electrically isolated, the current will be shared by two ducts (one intake duct and one exhaust duct), resulting in a more diffuse current distribution at the injection point and therefore a lower voltage. It would require an unusual coincidence of six circumstances, including inconsistent construction practices, for a strike to the dehumidifier house to produce the same common-mode voltage as a strike to the exhaust vent, but under no circumstances could a strike to the dehumidifier house produce a higher voltage than a strike to the exhaust vent, under the same assumptions.

The surge impedance of a buried reinforced concrete structure is typically much lower than the surge impedance of the lightning protection system; usually, the lightning protection system can be ignored. In this case, the fraction of current carried by the lightning protection system is significant, and it must be calculated before a reasonable agreement between the analytical and the numerical results is obtained. The equivalent circuit for the bay, soil, and lightning protection system is shown in Figure 8. L_{bay} represents the total inductance of the bay walls, R_{bay} is the resistance from the bay floor to infinity, and $R(t)$ is the time-varying surge impedance of the buried lightning protection system conductors. According to Chen and Warne [14], for a step function waveform, the surge impedance of two identical semi-infinite buried cylindrical conductors connected in parallel is

$$R(t) = \frac{1}{2}\frac{\zeta_0}{2\pi} e^{-\sigma t/2\varepsilon} I_0\left(\frac{\sigma t}{2\varepsilon}\right)\sqrt{\Omega_s \Omega_I} \rightarrow \frac{1}{2\pi\sigma\delta}\sqrt{\frac{\Omega_s \Omega_I}{\pi}}$$

where ζ_0 is the intrinsic impedance of free space, σ and ε are the conductivity and permittivity of the soil, respectively, I_0 is a modified Bessel function, and where

$$\Omega_s = \frac{1}{2}\ln\left(\frac{4t}{\mu\sigma a^2}\right) = \ln\left(\delta/a\right),$$

$$\Omega_I = \ln\left(\frac{2t}{\mu\sigma a d}\right) - \gamma = \ln\left(\frac{\delta^2}{2ad}\right) - \gamma,$$

$$\delta = \sqrt{\frac{4t}{\mu\sigma}}.$$

In the above equations, γ is Euler's constant ($\gamma = 0.57721...$), a is the radius, and d is the depth of the buried wire.

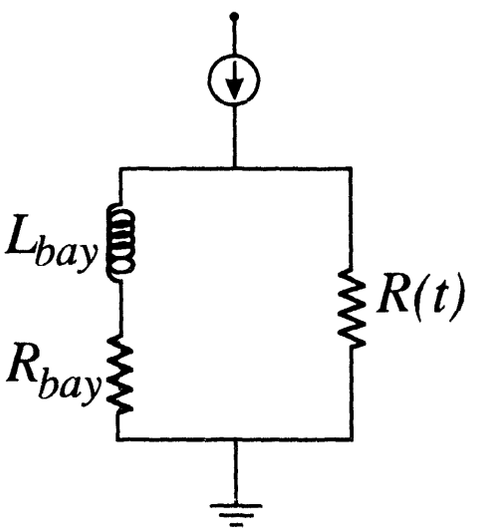

Figure 8. Equivalent circuit for the 12-64 bay analysis, which includes the effects of the bay, soil, and lightning protection system

To obtain the fraction of the lightning current diverted by the lightning protection system, an estimate of the resistance R_{bay} is needed. The resistance to infinity of the bay floor is approximately equal to the resistance of a buried hemisphere, whose radius is determined by equating the surface area of the bay floor to the surface area of the hemisphere. The resistance is

$$R_{bay} = \frac{1}{2\pi\sigma b},$$

where b is the radius of the equivalent hemisphere. Neglecting the inductive reactance of the wall rebar, the fraction f of the total current flowing in the lightning protection system is

$$f = \frac{R_{bay}}{R_{bay} + R(t)} = \left[1 + \frac{b}{\delta}\sqrt{\frac{\Omega_s \Omega_I}{\pi}}\right]^{-1}.$$

For a lightning pulse whose leading edge can be approximated by a squared sinusoid, if the 10-to-90 percent rise time is 0.3 μs, the maximum value is attained at 0.5 μs and the maximum rate of rise of the input current is at 0.25 μs, which is when the assembly area experiences its greatest potential difference. At 0.25 μs, the skin depth δ is 7.28 m, assuming σ = 0.015 S/m. The outer dimensions of the floor of the small bay are 27' by 31', resulting in an equivalent radius b of 3.52 m. Substituting a = 0.186" and d = 1', yields Ω_s = 7.34, Ω_I = 9.24, and f = 0.31.

Assuming the exhaust vent is well bonded to the reinforcing steel at the bay wall, the surface current spreads with a $1/\rho$ distribution. The internal electric field is the product of the surface current density and the surface impedance, and the internal voltage is the integral of the electric field. Carrying out the indicated operations, the result can be cast in the form of an effective inductance, L_{eff}, which multiplies the derivative of the total current,

$$L_{eff} = \frac{\mu_0}{2\pi} s \ln\left(\frac{s}{2\pi a}\right) \frac{1}{2\pi} \ln\left(\frac{h}{r_{duct}}\right),$$

where s is the spacing between vertical rebar, a is the radius of the rebar, h is the height of the roof above the floor, and r_{duct} is the radius of the ventilation duct. The calculation is complicated by the fact that the reinforcement in the side wall is not the same as the reinforcement in the back wall. There are also differences between the inside and outside layers. The approach was to consider the inside and outside layers separately and compute the inductance of the side-wall in parallel with the inductance of the back-wall using a straight forward modification of the preceding formula. Then the total transfer inductance of the wall is the parallel combination of the resulting "inside" and "outside" inductances, L^i and L^o. Using Figure 4, L^i evaluates to 16.23 nH and L^o evaluates to 35.32 nH. Finally, the peak voltage from the floor to the ventilation duct is given by

$$V_{\max} = \frac{L^i L^o}{L^i + L^o}(1 - f)\left.\frac{\partial I}{\partial t}\right|_{\max},$$

which accounts for the fraction of the current diverted by the lightning protection system. Substituting for L^i, L^o, and f, and assuming $\partial I/\partial t$ = 360 kA/μs gives a maximum voltage of 2.76 kV. The analogous voltage for one of the large bays is 2.56 kV.

6.4 Cell Analysis

Because of the difficulty in assigning a reduction factor for the fraction of current reaching the cell as the result of a strike to the top of the gravel mound, the full lightning current is assumed to be injected directly onto the cell walls at the worst possible point, namely, at the top inside edge of the ring beam (see Section 6.1). The current flowing out from the source point assumes a $1/\rho$ distribution, which, when integrated over the surface of the wall, yields the appropriate geometrical factor to scale the surface impedance. The inductance of the wall is therefore

$$L_s^{tot} = \frac{1}{2}\frac{\mu_0}{2\pi} s \ln\left(\frac{s}{\pi d}\right)\frac{1}{2\pi}\ln\left(\frac{h}{s}\right)$$

where d and s are the diameter and spacing between vertical rebar, respectively, h used in the formula is the height of the ring beam above the floor, and the leading factor of one-half is due to the two layers of rebar in the wall. The inner radius for the integration was assumed to be the distance from the strike point to the interior penetration area, which is also the same as the rebar spacing. Substituting the values s = 12 in., d = 0.5 in., and h = 21.5 ft yields L_s^{tot} = 30.3 nH and a maximum voltage of 10.9 kV.

7. Numerical Results

7.1 Approach

The numerical algorithm is the leapfrog finite-difference technique in the time domain. In this scheme, the Electric and Magnetic fields are assumed to be known at discrete points on two offset rectangular grids, and the fields between these points are assumed to vary as linear functions of the spatial coordinates. The three-dimensional grid where the Magnetic field is defined subdivides the problem space into rectangular solids, or cells, over which the medium is assumed to be uniform. The spatial and temporal partial derivatives in Maxwell's Equations are replaced by central differences, so that the resulting accuracy of the solution is order Δt^2 in time and Δx^2 in space. Starting with zero initial fields, and assuming a filamentary current source to simulate the lightning return stroke, the solution proceeds by calculating updated values of the Electric field in terms of spatial derivatives of the Magnetic field one-half step earlier in time, and vice versa. The particular finite-difference code used in the simulation was originally developed by Merewether and Fisher [15] and later extended to allow the modeling of more complicated geometries. Because of the influence of the original code, the new code has retained the name of its predecessor, THREDH.

7.2 PATRAN Interface

To input and validate the vast amounts of geometrical data that must be described to the computer for this type of simulation, a PATRAN-to-THREDH interface was developed. In this paradigm, PATRAN, a commercial geometrical modeling tool, is used to input the geometry information, complete with material parameters (ε, μ, σ), current sources, and a template for generating the finite-difference mesh. This information is output to a well documented, neutral-format ASCII file that is read by the interface routine. The function of the interface routine, called PAT3DH, is to discretize PATRAN's smooth mathematical representations of the lines, surfaces, and solids onto the rectangular finite-difference mesh, and to generate a new neutral file to allow the user to verify the results of the discretization visually in PATRAN. PAT3DH also produces a THREDH-readable input geometry file that contains a description of the finite-difference mesh, the

discrete geometry, the constitutive parameters (ε, μ, σ) for each cell in the mesh, surface impedances, transfer impedances, wire locations and radii, and the locations and orientations of perfect electric conductors. At lightning frequencies, common metals are accurately approximated by perfect electric conductors, where $\mathbf{E}^{tan} = 0$.

7.3 Modeling Guidelines

The resolution of a classical finite-difference approach is of the order of a grid spacing. Therefore, to model the rebar, which is one of the most important electrical features of a reinforced concrete structure, requires a grid spacing that is comparable to a rebar diameter. For a realistic structure, such as an assembly bay at Pantex, it is soon apparent that at one cell per rebar diameter, the size of the bay relative to the grid sizing and therefore the amount of computer memory required are so great that the problem cannot be solved by any existing computer, nor by any supercomputer envisioned in the next decade. For this reason, a means of modeling small details such as thin wires was developed for this class of computer codes.

7.4 Thin-Wire Algorithm

The approach behind the thin-wire algorithm is to assume electrostatic field distributions around the wire (rebar) and to derive local transmission line parameters, R, L, G, and C by applying Maxwell's equations in integral form to suitably chosen contours around the wire. The transmission line is then coupled to the external fields in the mesh in a self-consistent manner. Unfortunately, this leads to a weak numerical instability that is particularly troublesome in lightning simulations, where the number of time steps is typically very large.

The technique in THREDH for suppressing the numerical instability is one due to Godfrey [16,17] for reducing numerical noise in a particle-in-cell code. In his technique, the Electric field **E** is written in terms of the average of the spatial derivatives of **H** at both the previous and future half time steps. The effect of the average is to smooth the Magnetic field before supplying it the **E**-advance equation. The equation for advancing **H** in terms of **E** is unchanged. The usual leapfrog method is explicit, that is, unknown quantities are determined entirely in terms of known quantities. Godfrey's method is implicit, in which unknowns appear on both sides of the equations. The resulting system of equations is solved by iterating back and forth between the equations for advancing **E** and **H** using the Magnetic field at the previous time step as an initial guess for the future Magnetic field. The fields are typically slowly varying in lightning problems so that this is an excellent first approximation, and the iteration process typically converges in four steps.

7.5 Rebar Modeling — Thin-Wire Approach versus Transfer Impedance

There are two possible approaches for modeling the large number of reinforcing bars in the concrete walls, roof, and floor of the assembly areas at Pantex. The first approach is to model each section of rebar by the thin-wire algorithm. This approach has the advantage that fine details, such as the connection of an air terminal or ground loop to the reinforcing bars, or the penetration of a conduit through the wall or floor, are treated naturally. A disadvantage is that the grid spacing is limited by the spacing between rebar, which may in turn require a large number of grid points and a correspondingly small time step. For realistic problems, two cells per rebar spacing (as opposed to four, which is 16 times as expensive), is a practical upper bound on the accuracy that can be achieved. A second disadvantage is that the memory required to store the wire data for typically 100,000 sections of rebar is significant.

The second approach to rebar modeling is the transfer impedance method, in which the reinforced concrete walls are replaced by perfect conductors to obtain the surface current density on the walls, which is then multiplied by the analytical transfer impedance to obtain the electric field inside the bay or cell. This electric field, when integrated from the floor to the ceiling in the plane of the lightning flash, yields the maximum open-circuit voltage available for driving internal circuits. This approach has the advantage that the mutual coupling between individual rebar is computed very accurately. It also requires fewer grid points than the thin-wire algorithm, because the grid spacing is not limited by the spacing between rebar. The disadvantages are that the transfer impedance method smoothes out fine details near penetrations, attachment points, grounding points, and bonding connections, and that it requires a complicated correction near edges and sharp corners.

With either method, no more than 20% accuracy can be expected with current computers for this class of problem.

7.6 Lightning Source Modeling

A return stroke is a wavelike disturbance on what is essentially a charged transmission line. The disturbance results from the closing of a switch between the charged line and the point of strike. Unfortunately, simulating the pre-strike static Electric field is extremely difficult because of the limited volume that can be accommodated in the finite-difference problem space. The charges associated with a realistic return stroke, when confined to the limited surface areas in the finite-difference volume, result in such an enormous static Electric field that it dominates the responses of interest. In the absence of a better approach, the present guideline for simulating a lightning return stroke is that the current must have a return path. This approach has been validated in triggered lightning tests of a buried munitions storage igloo [18].

The lightning sources used in subsequent calculation are variations of the following. A column of current sources is assumed to extend vertically upward from the attachment point to a point three and a half cells inside the outer boundary. At this point, the source wire splits into four perpendicular wires, each carrying one fourth of the total return stroke current. Each of the four wires extends from the common point of intersection to a point three and a half cells inside the vertical boundary, at which point the wire turns downward and connects to the inside of a perfectly conducting cup that surrounds the soil. The fall times of lightning return strokes are typically 50 μs, but because the interior voltages respond primarily to the time derivative of the input current waveform, a short-duration input waveform is sufficient to establish the peaks. Again, because the interior voltages respond to $\partial I/\partial t$, any combination of amplitudes and rise times with a maximum rate of rise of 360 kA/μs would produce the same upper bound. The results in this report have been computed assuming an amplitude of 120 kA and a rise time of 0.3 μs.

7.7 Bay Simulation Results

Because the analysis showed that a lightning strike to a small bay results in a higher common-mode voltage than a strike to a large bay, a small bay was chosen for the numerical simulation. The bay walls and roof are insulated from the soil by a 4" layer of polystyrene plastic, so that the effect of neighboring bays is minimal; only the bays immediately adjacent to the bay under consideration were modeled in the simulation. As assumed for the analytical estimate, the attachment point was on an air terminal on the exhaust vent in the corner of the bay. Two dehumidifier houses, with their lightning protection systems were included in the computer model,

as well as 238' of ramp on both sides of the 12-64 complex. Because of discretization error, the polystyrene layer on the roof and walls of the bay was 6" thick. The lightning protection conductors and static ground wire were also included.

The problem space measured 253' from east to west, 203' from north to south, and 126' vertically. This allowed 20' of clearance between the ramp and the outer boundary, roughly 65' of soil below the bottom of the bays, 35' of air from the tops of the bays to the outer boundary, and more than 100' of lightning protection conductors and ramps on both sides of the lightning channel. The volume was discretized to produce an exponentially expanding and contracting grid as needed to provide the finest resolution near the bay of interest and, to reduce computation time, less resolution away from the bay of interest. The minimum grid spacing was 1'; the maximum grid spacing was 5'. The number of cells was 141 by 141 by 64. A CAD drawing of the computer model is shown in Figure 9.

For this simulation the rebar was modeled using the transfer-impedance method, in which the walls were replaced by perfect conductors for the purpose of obtaining the current density, which was then multiplied by the transfer impedance to obtain the internal Electric field. The integral of the Electric field from the floor to the ventilation duct results in the maximum common voltage. For this simulation, the conductivity and relative permittivity of the soil were assumed to be 0.015 S/m and 30, respectively.

Three simulations were performed with different instability-suppression schemes, boundary conditions, and lightning source networks. For any two simulations, the peak common-mode voltages computed by the finite-difference code differed by at most six percent. A plot of the median-amplitude voltage waveform from the three finite-difference runs is shown in Figure 10, overlaid with the analytical upper bound. The peak amplitude of the numerical result is 2.28 kV.

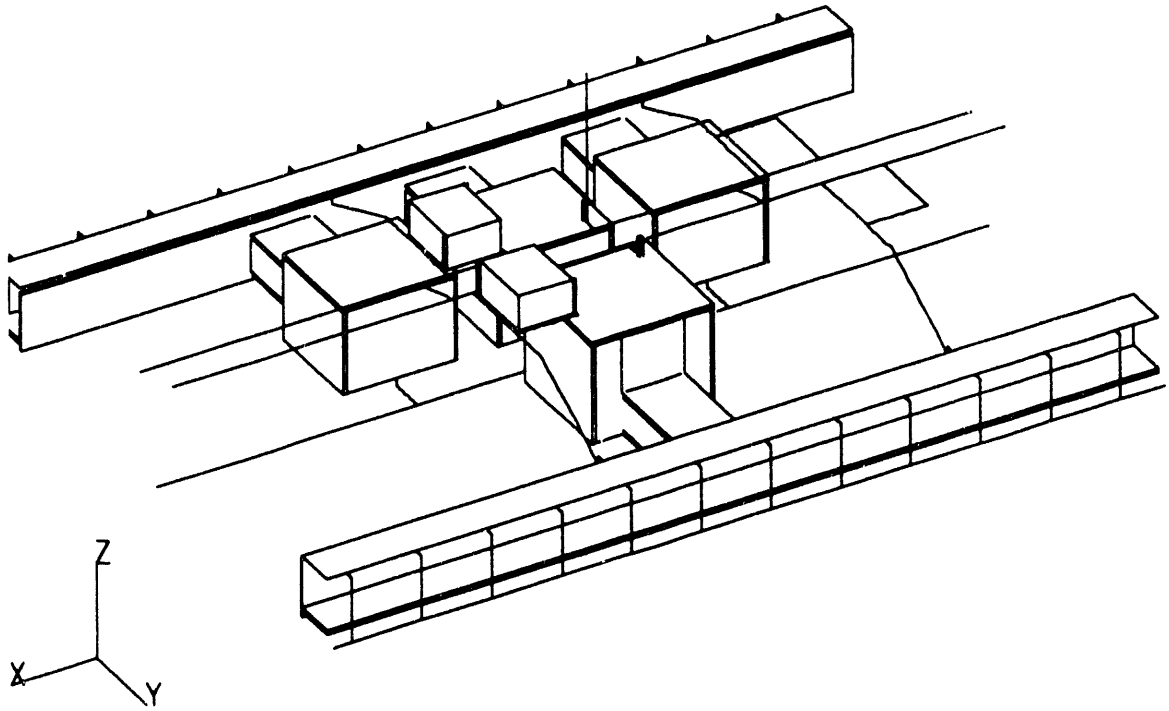

Figure 9. Computer model for the 12-64 numerical simulation

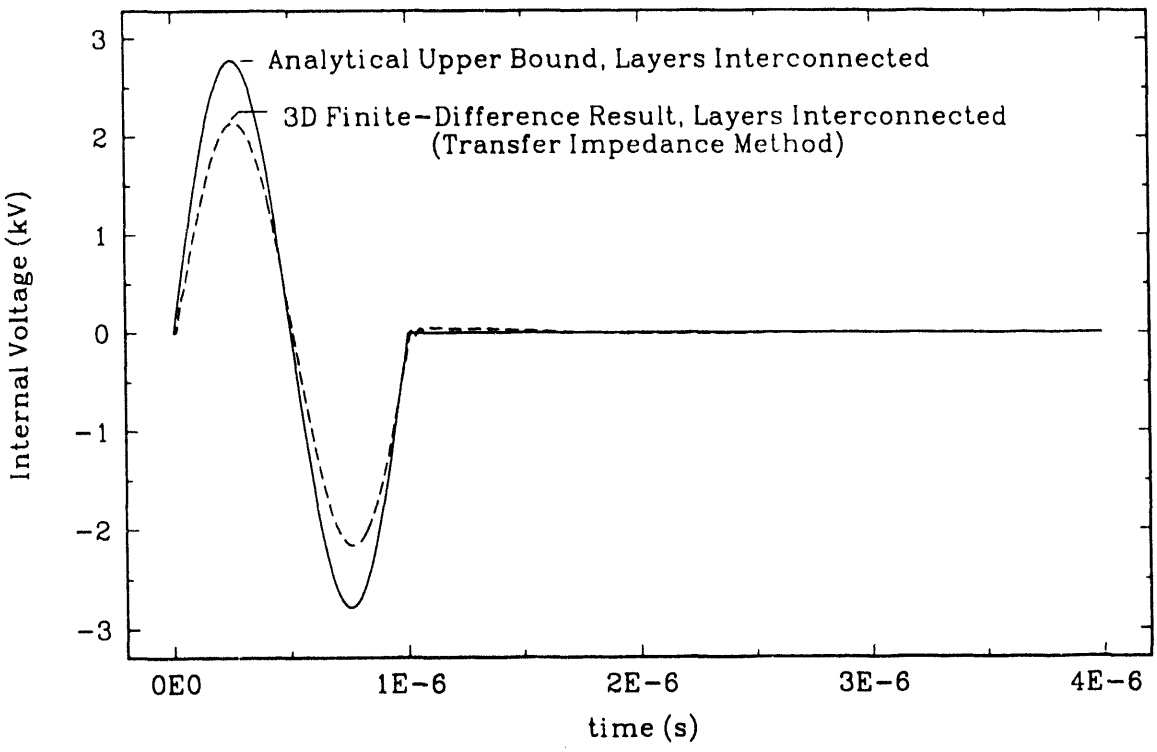

Figure 10. Median-amplitude voltage waveform obtained from three numerical simulations of Building 12-64 together with the analytical upper bound

As an aside, the fraction of the total lightning current diverted by the lightning protection system at the ventilation duct was calculated to be 24 percent, compared to the analytical estimate of 31 percent calculated in Section 7.3. Some difference was expected because of the approximations involved in both the analysis and the numerical simulation.

7.8 Cell Simulation Results

To treat the effect of the ramp more accurately, the cell analysis was conducted in two steps. In the first step, called the site analysis, a coarse finite-difference grid was adopted to include large amounts of soil around the cell and long lengths of the 12-44 ramp. The ramp was terminated one cell away from the perfectly conducting cup at both ends to reduce reflections at the outer boundary. Ramp bulk currents on both sides of the equipment passageway were accurately monitored with the intention of supplying these currents as current sources in the second step of the analysis, called the building analysis. In the building analysis, a much more refined finite-difference mesh is used to resolve the field variations in the walls and near geometrical details in the cell that may be important. At places where the ramp or other long conductors would have penetrated the outer boundary in the refined analysis, the conductors are connected to the return circuit by current sources whose values were determined during the site analysis.

The problem space for the site analysis measured 365' by 707' by 172', which allowed for 100' of clearance from the cell walls to nearest boundary, 689' of ramp, 100' of soil below the cell floor, and 36' of air above the gravel mound. For a current injected directly on the cell wall, the resulting local current distribution is not affected significantly by the presence of neighboring cells; therefore, only one cell was modeled in the simulations. All concrete and air trapped in the interlocked passageways, corridors, and round room were given the properties of perfect conductors. The region was discretized onto a nonuniform mesh with a minimum grid spacing of 3' and a maximum grid spacing of 6', so that the finest resolution was obtained in and around the cell itself, while fewer unknowns were used at large distances from the cell. The resulting finite-difference grid was 84 by 132 by 43. A CAD drawing of the site analysis geometry with its source network is shown in Figure 11. The soil conductivity and relative dielectric constant were assumed to be 0.015 S/m and 30, respectively.

Figure 12 shows the bulk currents on the ramp at the two places where the ramp penetrates the outer boundary in the refined building analysis. Their peak amplitudes are +3.60 kA at 0.66 μs and -4.41 kA at 0.68 μs for a 120-kA input current with a 0.3-μs rise time.

For the second step of the analysis, the round room rebar was modeled with the thin-wire algorithm. The walls, roof, and floor of the mechanical room, cubicles, staging area, corridors, and passageways were modeled by perfect conductors (the surface impedances of the reinforced concrete walls, floors, and roofs are low enough that their macroscopic current distributions are the same as those on perfectly conducting surfaces). The problem space measured 155' by 115' by 85'. The cell walls and gravel mound were about 20' from the outer boundary on all sides, and there were 30' of soil below the cell. The volume was superimposed on a nonuniform mesh with a minimum grid spacing of 6" and a maximum grid spacing of 2.5', so that the number of grid points numbered 178 by 127 by 62. The constitutive parameters of the soil, ε_r, μ_r, σ, were assumed to be 30, 1, and 0.015 S/m, respectively; the constitutive parameters of the gravel were assumed to be 30, 1, and 10^{-6} S/m, respectively; and the constitutive parameters of the concrete were assumed to be 50, 1, and 0.01 S/m, respectively. Figure 13 shows the PATRAN model developed for the refined cell analysis.

Figure 14 shows the common-mode voltage inside the cell for this geometry, compared to the analytical upper bound. The bipolar, derivative character of the numerical result indicates that the inductance of the wall is playing the major role in determining the interior voltage; the broadening of the waveform is dispersion caused by the soil. The peak value of the numerical result is 5.4 kV. Figures 15 and 16 show the electric and magnetic field intensities in a cross section of the cell containing the source current. The contours are labeled with the common logarithms of the electric and magnetic field magnitudes, in V/m and A/m, respectively.

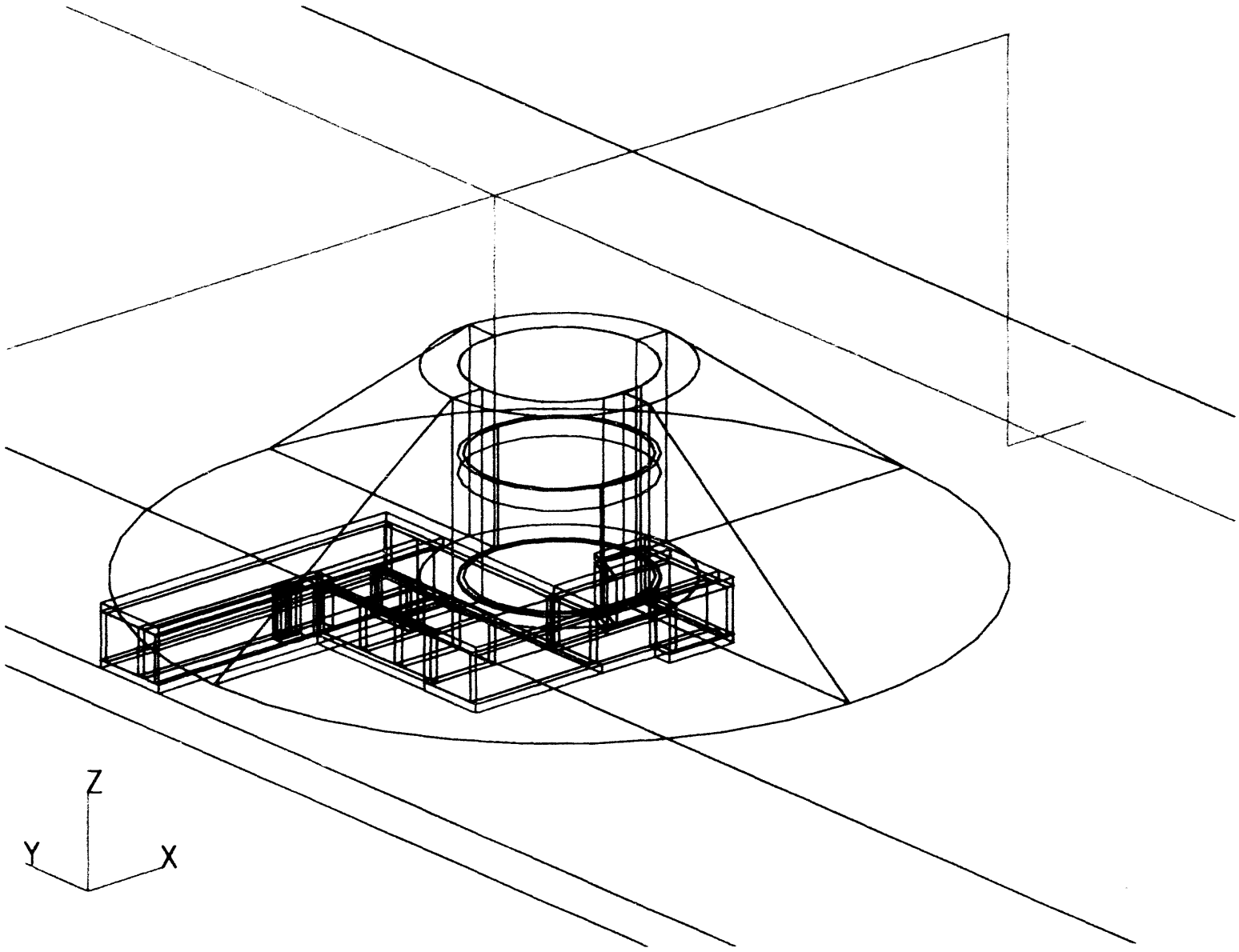

Figure 11. Cell site analysis geometry, showing the lightning source network that provides the return path for the lightning current

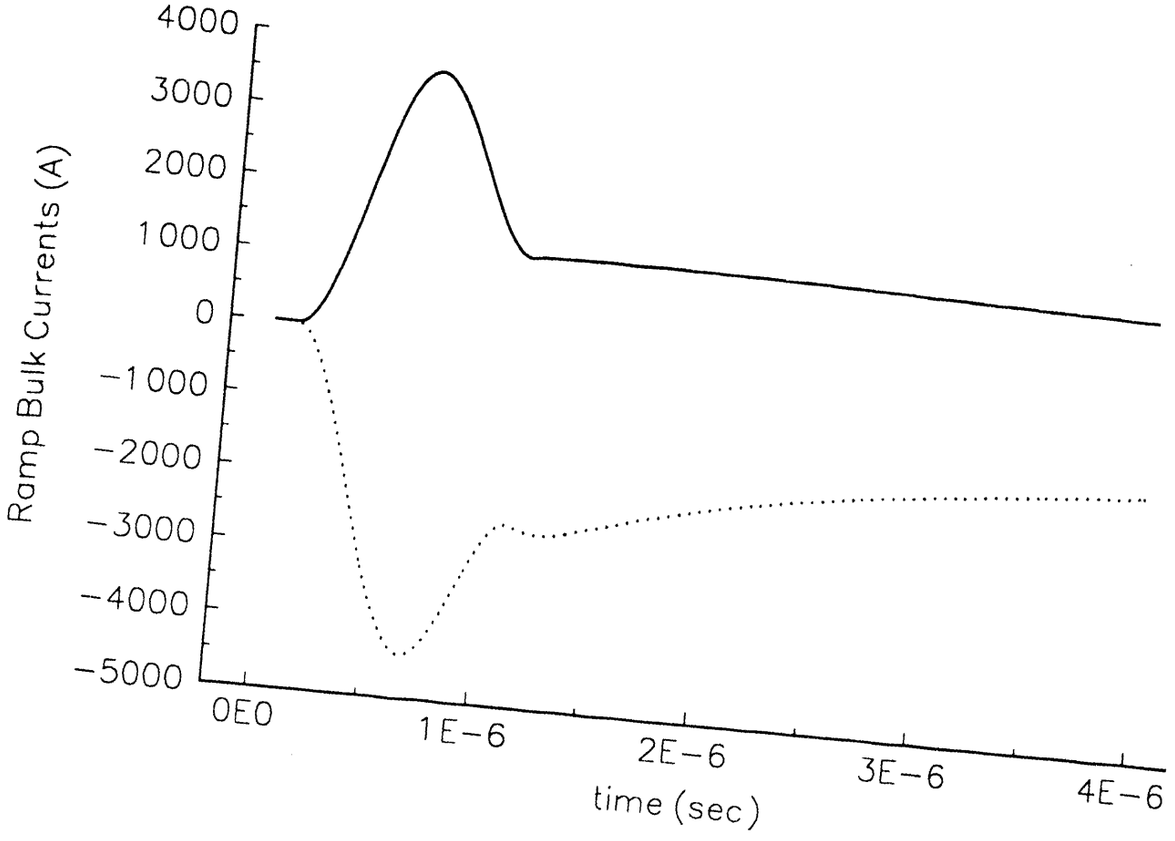

Figure 12. Ramp bulk currents computed in the cell site analysis

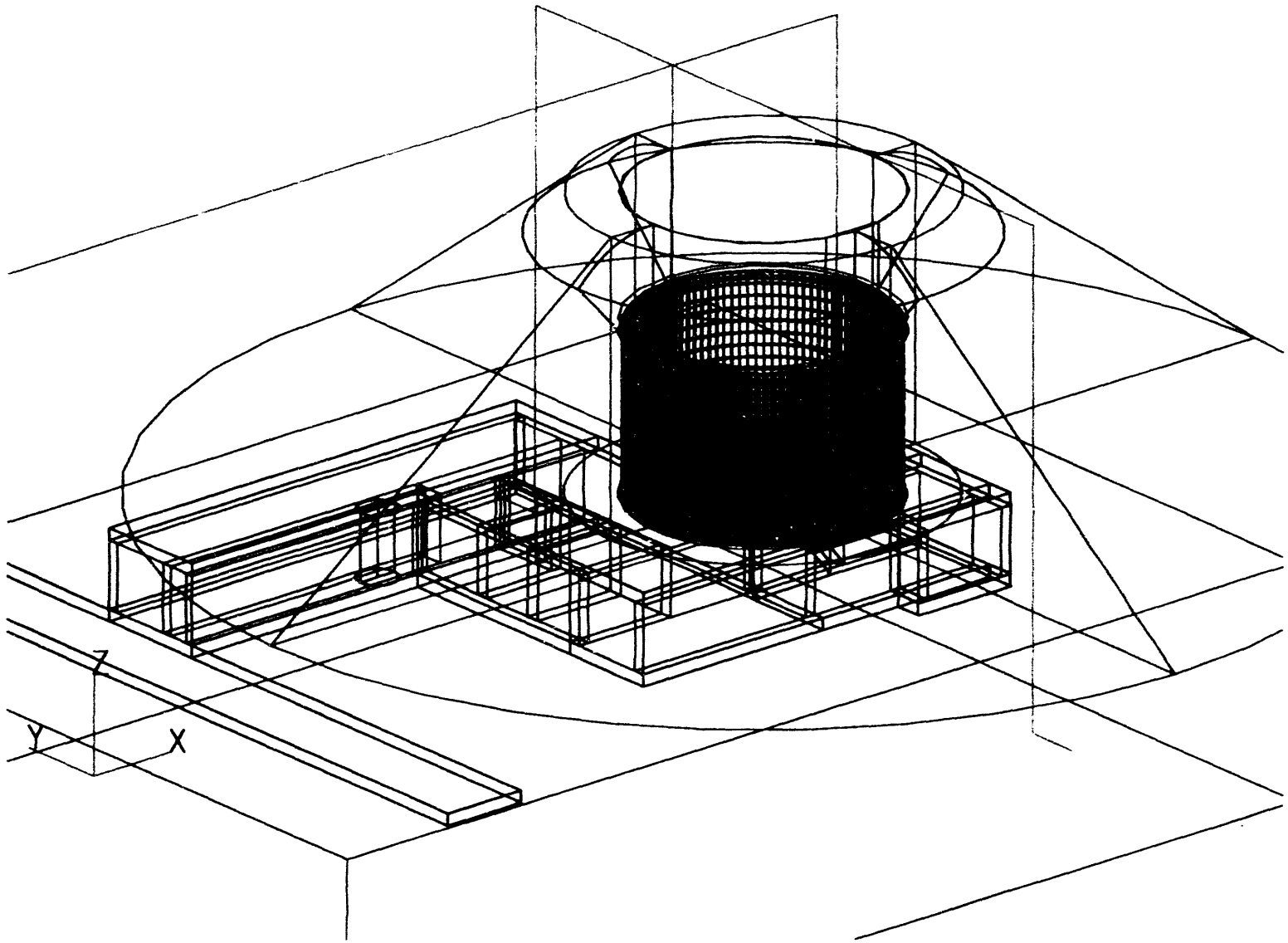

Figure 13. CAD model of 12-44 cell (thin wire approach)

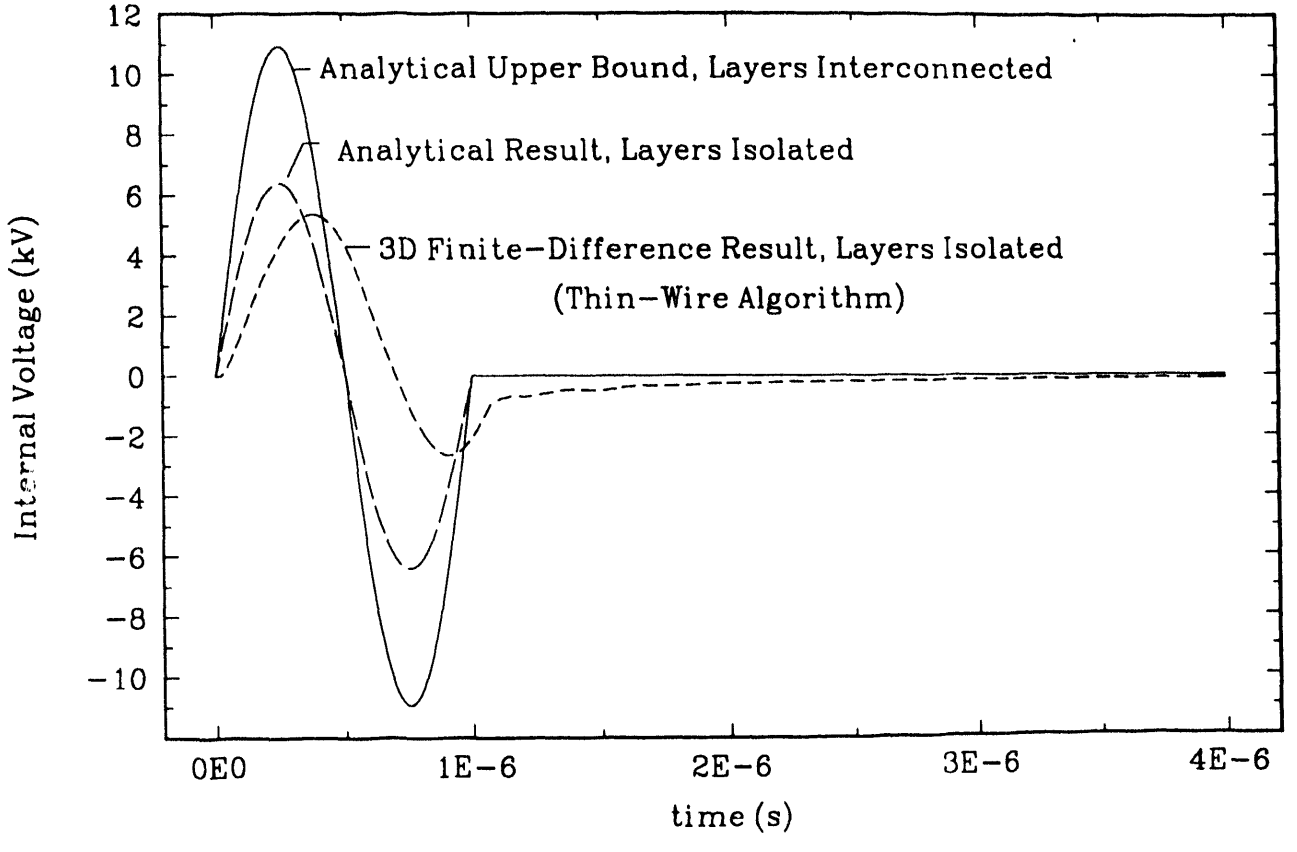

Figure 14. Maximum common-mode voltage in a 12-44 cell due to severe lightning, with two analytical estimates

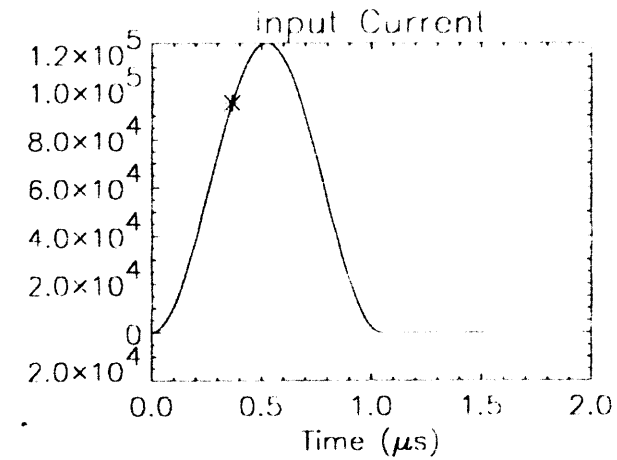

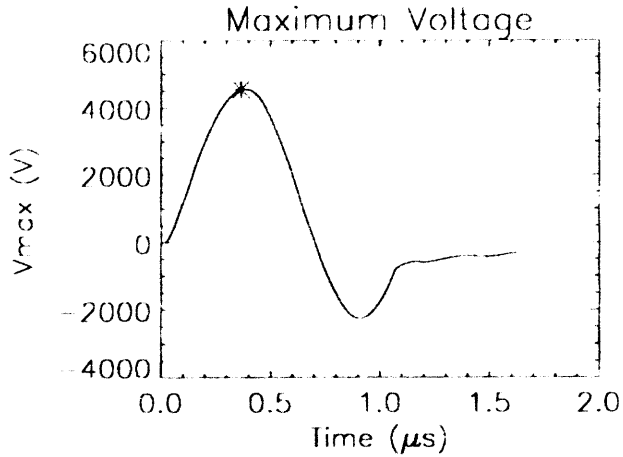

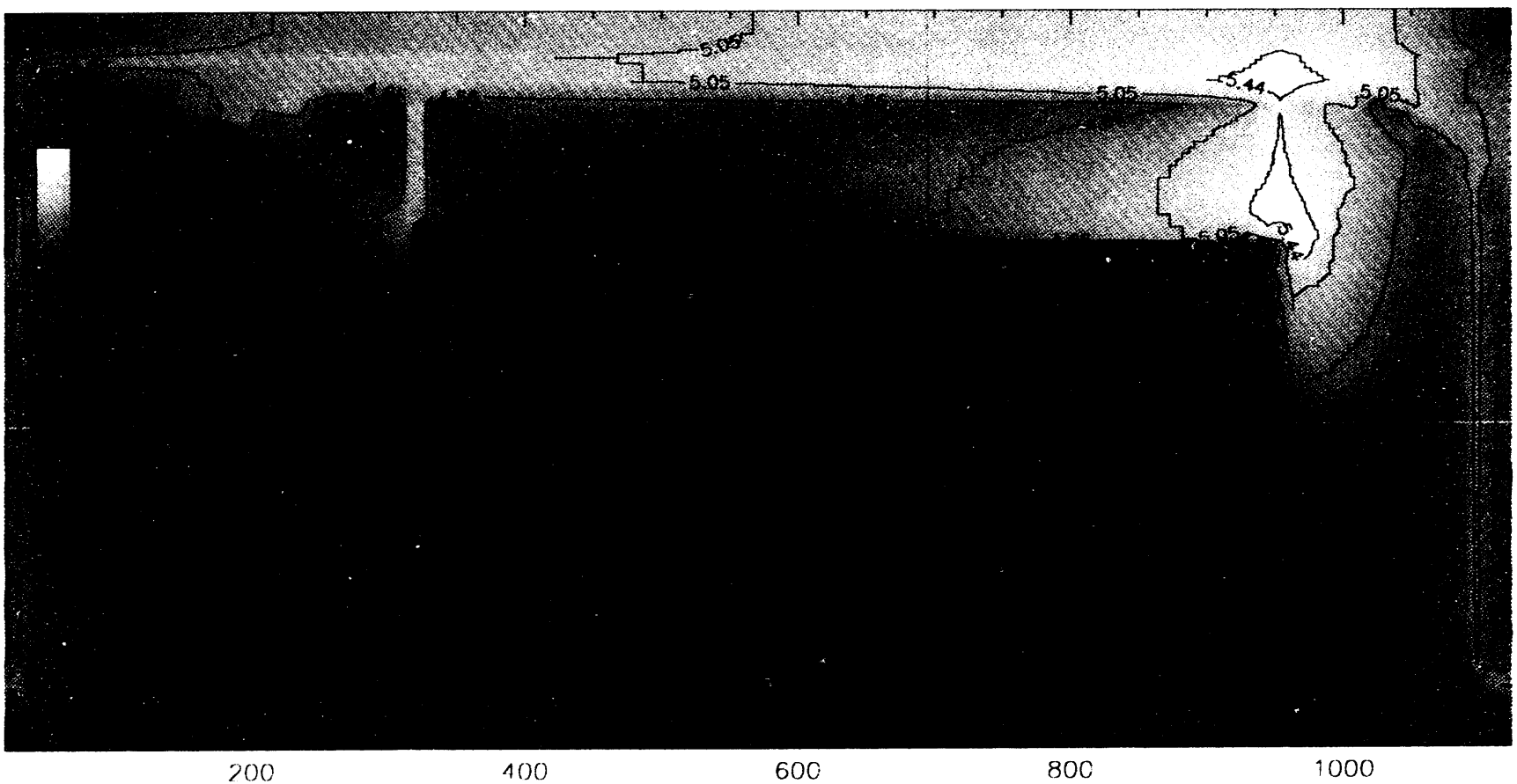

Figure 15. Electric field cross section in a 12-44 cell due to a lightning current with a 360 kA/μs maximum rate of rise (A contour labeled 2.72 means that the magnitude of the electric field is $10^{2.72}$ on that contour)

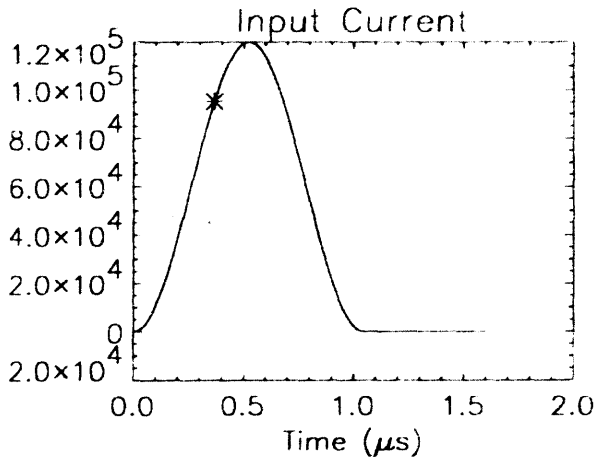

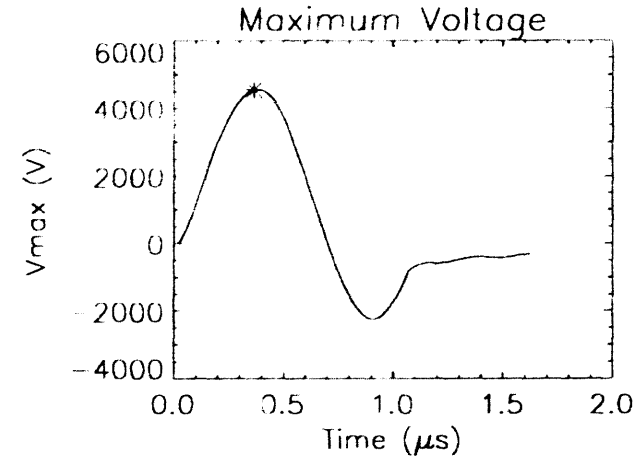

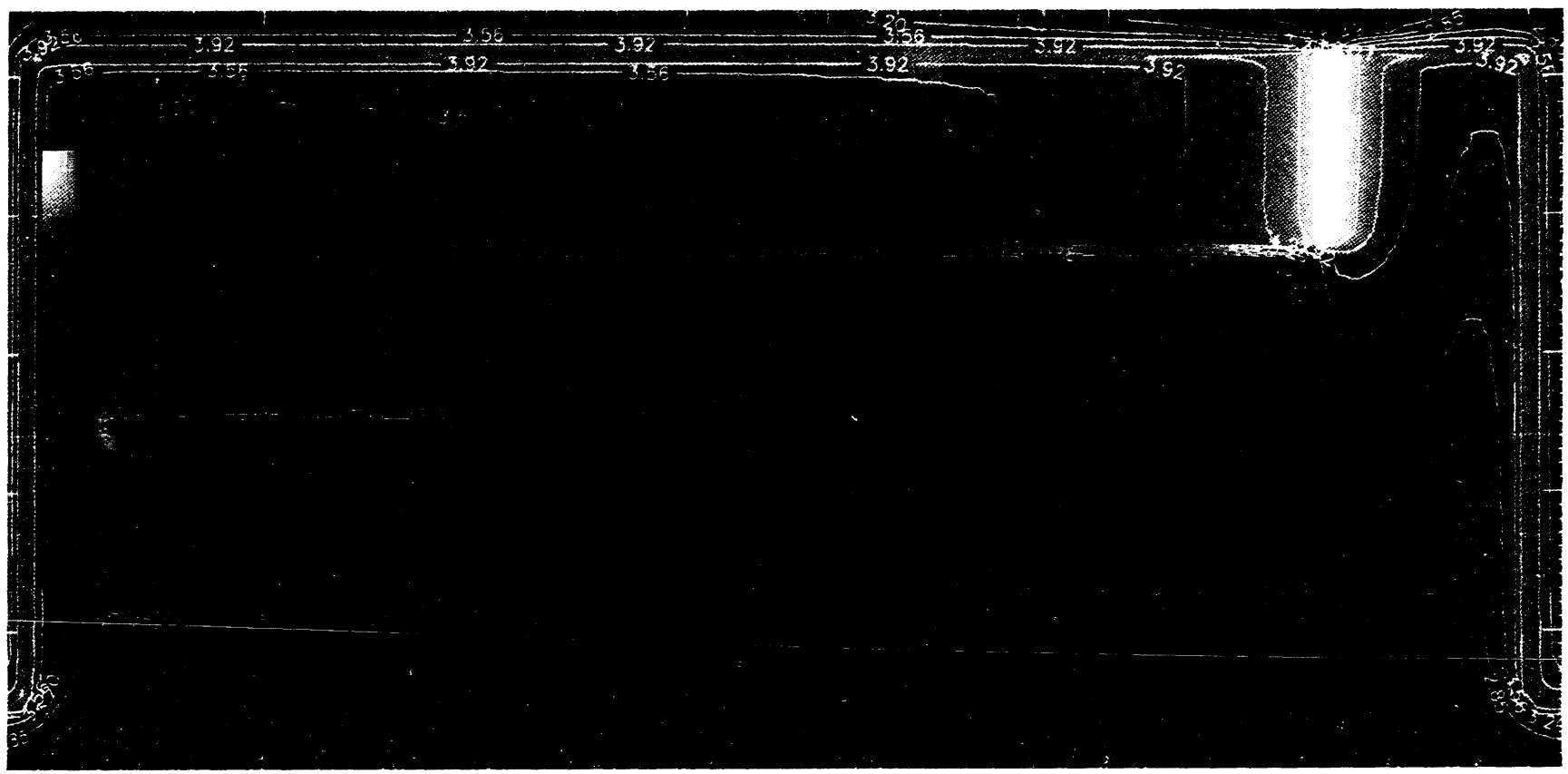

Figure 16. Magnetic field cross section in a 12-44 cell due to a lightning current with a peak amplitude of 120 kA

8. References

[1] Morris, M. E, and K. C. Chen, AC Power Line Surge Protection for Critical Assembly Areas at Pantex, Sandia National Laboratories memorandum to Kenneth Pierce, October 21, 1991.

[2] Seely, G. A., and P. Holmes, *Rebar Junction Contact Resistance*, Electromagnetic Test Report, Electromagnetic Analysis and Test Department, Sandia National Laboratories, Albuquerque, NM, May 1993.

[3] Solberg, J. E., and P. Holmes, *Pulse Tests on Pantex Surge Suppressors*, Electromagnetic Analysis and Test Department, Sandia National Laboratories, Albuquerque, NM, February 1993.

[4] Weidman, C. D., and E. P. Krider, "The fine structure of lightning return stroke waveforms," *J. Geophys. Res.*, **83**:6239-6247 (1978). Correction, *J. Geophys. Res.*, **87**:7351 (1982).

[5] Weidman, C. D., and E. P. Krider, "Submicrosecond rise time in lightning return stroke fields," *Geophys. Res. Lett.*, 7:955-958 (1980). Correction, *J. Geophys. Res.*, **87**:7351 (1982).

[6] Plumer, J. A, editor, *Lightning Protection for Facilities and Electrical/Electronic Systems*, Pittsfield, MA, pp. 4-5 through 4-11.

[7] Viemeister, P. R., *The Lightning Book*, Doubleday, New York, 1962.

[8] Jones, R. D., *EM Environmental Hazards Resulting from Lightning at the Pantex Facility*, Sandia National Laboratories internal memorandum to Parker F. Jones, January 15, 1976.

[9] *NFPA-78 Lightning Protection Code*, National Fire Protection Association, Quincy, MA, 1989, p. 33.

[10] Changery, M. J., *National Thunderstorm Frequencies for the Contiguous United States*, U.S. Nuclear Regulatory Commission, NUREG/CR-2252, November 1981.

[11] Cianos, N., and E. T. Pierce, *A Ground-Lightning Environment for Engineering Usage*, Stanford Research Institute Technical Report L.S.-2817-A3, Menlo Park, CA, 1972.

[12] Lee, K. S. H., editor, *EMP Interaction: Principles, Techniques, and Reference Data*, revised printing, Hemisphere, 1986, pp. 464-470.

[13] Merewether, K. O., and K. C. Chen, *Analytical Estimates for the Maximum Voltages Inside Nuclear Assembly Areas at Pantex due to Direct Lightning, Interim Report*, Electromagnetic Analysis and Test Department, Sandia National Laboratories, Albuquerque, NM, February 1993.

[14] Chen, K. C., and L. K. Warne, Surge Impedances for Spherical and Cylindrical Structures, Sandia National Laboratories Internal Memorandum, Electromagnetic Analysis and Test Department, May 30, 1992.

[15] Merewether, D. E., and R. Fisher, *Finite-Difference Solution of Maxwell's Equations for EMP Applications*, Electro Magnetic Applications, Inc., EMA-79-R-4, Final Revision, Nov 16, 1982.

[16] B. B. Godfrey, *Proceedings of the Ninth Conference on Numerical Simulation of Plasmas*, Paper 0D-4.

[17] B. Goplen, R. E. Clark, J. McDonald, and W. M. Bollen, *User's Manual for MAGIC*, Mission Research Corporation, MRC/WDC-R-068, Alexandria, VA, 1983, Sec. 3, pp. 21-26.

[18] Merewether, K. O., and M. E. Morris, "Finite-difference analysis of a buried munitions storage bunker subject to direct lightning and comparison with experiment," *Proceedings of the Int'l Aerospace Conference on Lightning, Grounding, and Static Electricity*, Atlantic City, NJ, Oct 6, 1992.

Appendix A
Pantex Lightning Flash Data

In this appendix, actual lightning occurrence data from the local lightning detection system at Pantex are presented for comparison with the semi-empirical estimates given in Section 5. The visual display of the Lightning Location and Protection, Inc. (LLP) lightning detection system has been reproduced in Figure A-1, showing the Pantex plant and a rectangular area that includes Zone 12. Zone 12 itself is not mapped directly on this system.

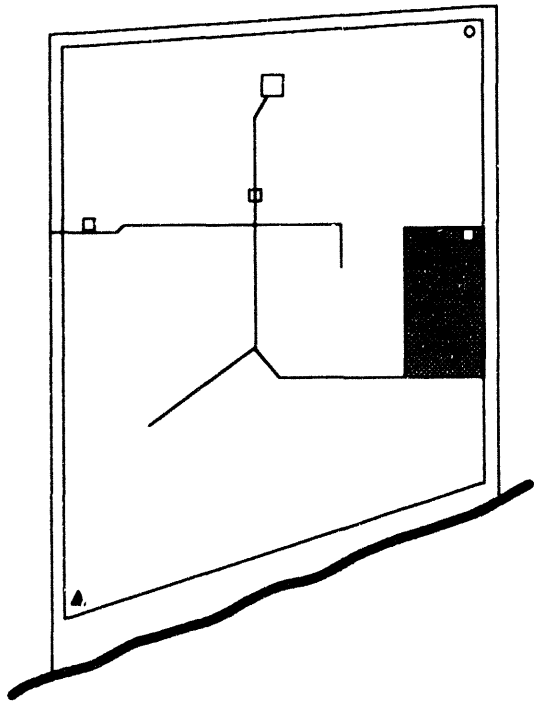

Figure A-1. LLP display of the Pantex plant. The shaded region is a rectangular area that includes Zone 12.

Table A-1 shows the number of lightning flashes, by month and year, to an area five miles in radius to the entire Pantex plant, and to this rectangular area. The system is designed to record only cloud-to-ground flashes. The last three rows of the table show the total number of flashes to each region over the three-year period, the average number of flashes per year to each region, and the corresponding estimates using the NRC isokeraunic map (T_y = 60 thunderstorm days per year) and the empirical formulas of Cianos and Pierce as described in Section 5. As is evident from the table, the estimates agree quite well with the actual data over this period.

Table A-1. Pantex Lightning Flash Data*

Year	Month	Five-Mile Radius (203.4 km^2)	On-Plant (45.3 km^2)	Rectangular Area (2.23 km^2)
1991	January	0	0	0
	February	0	0	0
	March	0	0	0
	April	2	1	0
	May	301	40	3
	June	311	37	3
	July	228	59	4
	August	2	0	0
	September	89	8	0
	October	3	3	0
	November	0	0	0
	December	2	0	0
1992	January	2	2	1
	February	0	0	0
	March	54	11	2
	April	229	49	3
	May	77	8	0
	June	752	140	7
	July	173	37	7
	August		Data not available	
	September	0	0	0
	October	0	0	0
	November	0	0	0
	December	0	0	0
1993	January	0	0	0
	February	0	0	0
	March	9	6	0
	April	26	3	0
	May	61	6	0
	June	177	41	0
	July	230	72	6
	August	304	74	5
	September	127	23	0
	October		Data not available	
	November		Data not available	
	December		Data not available	
Three-year Totals		3159	620	41
Averages (per year)		1053	207	13.6
Estimated (per year)		1012	226	11.1

*The authors are indebted to Linda Smith of Pantex for supplying the above data.

Distribution

1 U. S. Department of Energy, Headquarters
Attn: Tom Stephan, DP20.1
1000 Independence Avenue S. W.
Washington, DC 20585

4 U. S. Department of Energy
Amarillo Area Office
Attn: P. M. Ramey, Area Manager
Dick Phillips
P. O. Box 30030
Amarillo, TX 79120

2 U. S. Department of Energy
Nuclear Explosive Safety Division
Attn: E. R. Hanson
J. Paul Luette
P. O. Box 98518
Las Vegas, NV 89193-8518

3 U. S. Department of Energy
Albuquerque Operations Office
Attn: Frank Rider (NESD)
P. O. Box 5400
Albuquerque, NM 87115

11 Mason & Hanger - Silas Mason Co., Inc.
Pantex Plant
Attn: R. M. Loghry, General Manager
J. C. Drummond, Division Manager, Quality
T. F. Hall, Acting Director, ES&H/WM
P. O. Box 30020
Amarillo, TX 79177

3 University of California
Lawrence Livermore National Laboratory
Attn: R. L. Samuelson, L-575 (USDOE, SF - LLNL)
C. J. Anderson, L-142 (Mgr. NES)
T. K. Devlin, L-125 (Special Assistant for Weapons ES&H)
P. O. Box 808
Livermore, CA 94550

Distribution (Continued)

3 Los Alamos National Laboratory
Attn: L. M. Kelly, WX-DO, MS P945
W. J. Higgins, WX-1, MS C936
Rick Higgs, WX-DO
P. O. Box 1663
Los Alamos, NM 87544

1	MS 9006	E. E. Ives (Org. 5200)
1	MS 9005	J. B. Wright (Org. 5300)
1	MS 9033	C. A. Pura (Org. 5362)
1	MS 0447	J. O. Harrison (Org. 5115)
1	MS 0479	D. D. Tipton (Org. 5151)
1	MS 0490	S. D. Spray (Org. 12331)
1	MS 0490	W. E. Mauldin (Org. 12331)
1	MS 0492	J. P. Cates (Org. 12332)
1	MS 0492	G. A. Sanders (Org. 12332)
1	MS 0492	D. H. Loescher (Org. 12332)
1	MS 0492	J. A. Richardson (Org. 12332)
1	MS 0631	R. L. Schwoebel (Org. 12300)
1	MS 0632	J. L. Duncan (Org. 12303)
10	MS 0865	K. C. Chen (Org. 2753)
20	MS 0865	M. O. Merewether (Org. 2753)
1	MS 0865	R. D. Jones (Org. 2753)
1	MS 0872	P. A. Longmire (Org. 5407)
1	MS 1390	J. J. Schwartz (Org. 12364)
1	MS 9018	Central Technical Files (Org. 8523-2)
5	MS 0899	Technical Library (Org. 7141)
1	MS 0619	Technical Publications (Org. 7151)
10	MS 0100	Document Processing for DOE/OSTI (Org. 7613-2)

END

DATE
FILMED
3/4/94